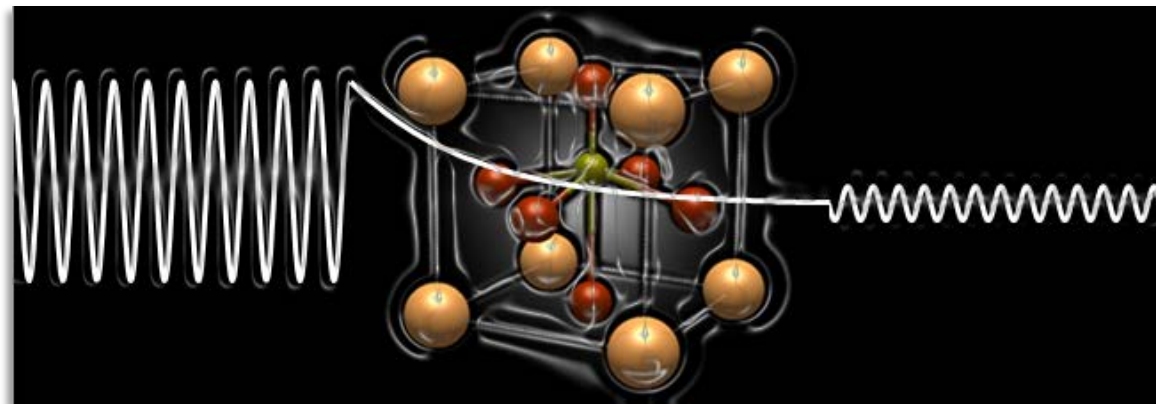




Spintronics with Ferroelectrics

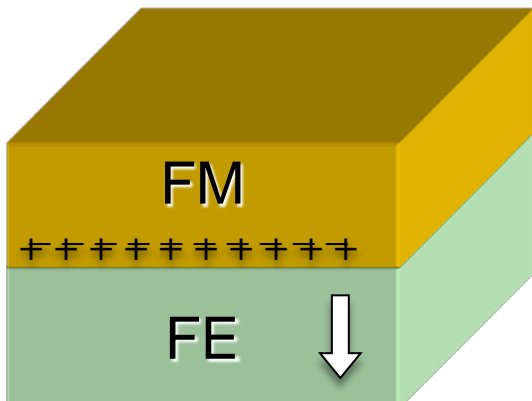
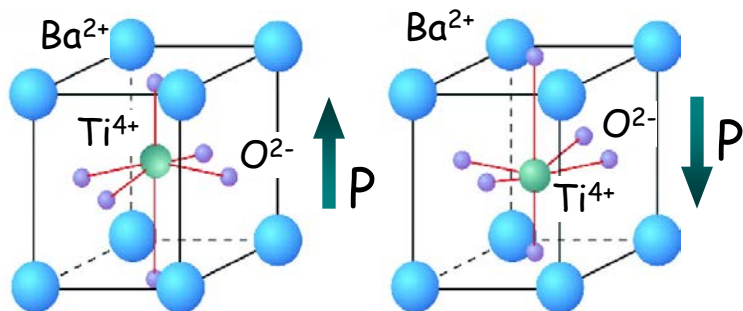
Evgeny Tsymbal

Department of Physics and Astronomy
Nebraska Center for Materials and Nanoscience
University of Nebraska-Lincoln



Ferroelectrics: Field Effect

Ferroelectric BaTiO_3



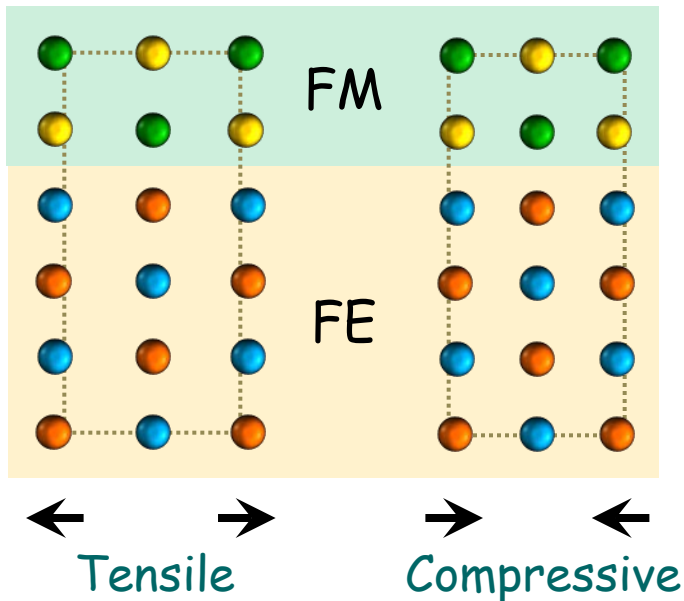
- Spontaneous electric polarization switchable by electric field
- Polar displacements $\sim 0.1\text{-}0.2\text{\AA}$
- Perovskite structure
- Large polarization charge:
 $10 - 100 \mu\text{C}/\text{cm}^2 (\sim 0.1 - 1 \text{ e}/\text{a}^2)$
- Polarization charge screening:
 "field effect". Effective electric fields up to $10 \text{ V}/\text{\AA}$ ($1 \text{ GV}/\text{cm}$)
- Controlled by fields of $\sim 1 \text{ MV}/\text{cm}$
 Three order in magnitude smaller!
- Non-volatile capability
- Control of spin-dependent properties relevant to spintronics



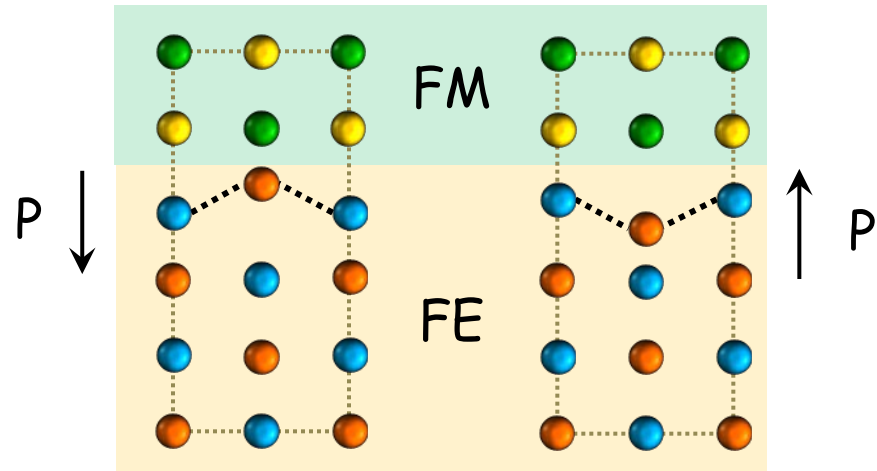
Ferroelectrics: Strain and Bonding

Ferroelectrically induced:

- Interface strain effects



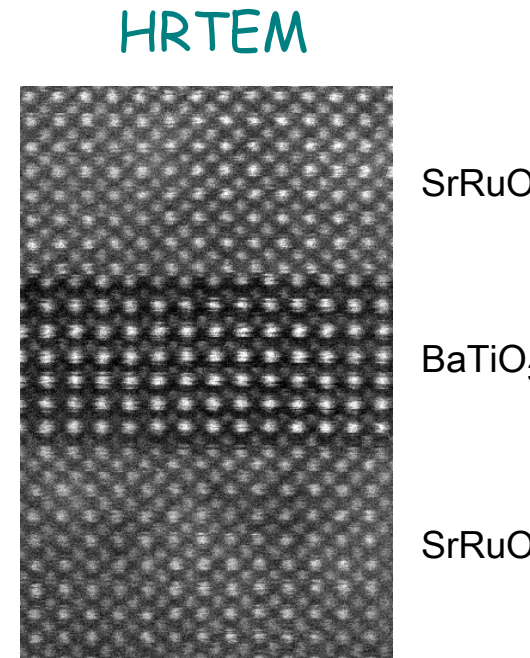
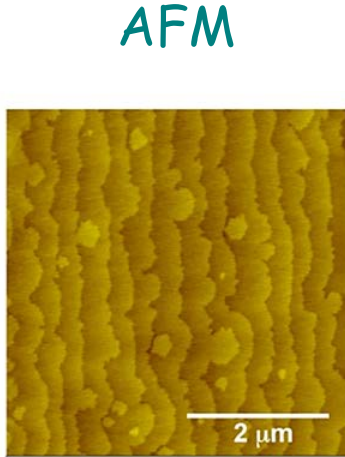
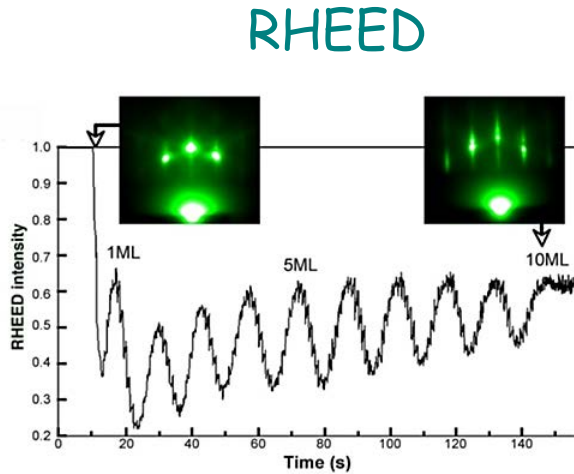
- Interface bonding effects





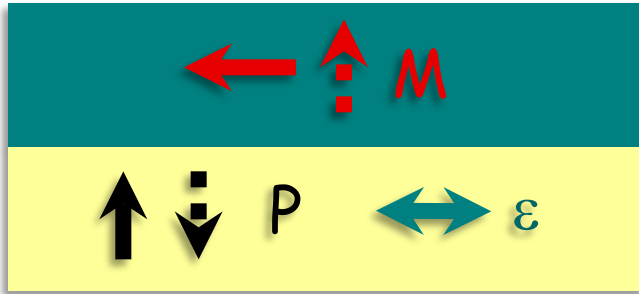
Ferroelectrics: Epitaxial Thin Films

- High quality epitaxial structures with nearly atomic precision interface control: PLD, MBE
- Epitaxial strain to stabilize polarization
- Stable and switchable polarization in sub nm thick films





Magnetoelectric Interfaces



Magnetic (Ferromagnetic, Ferrimagnetic, Antiferromagnetic)

Ferroelectric

- Strain mediated:
Piezoelectricity & Magnetostriiction or Piezomagnetism
- Electronically driven:
Spin-polarized screening or interface bonding
Effects of ferroelectric polarization on:
 - Interface magnetization
 - Magnetocrystalline surface anisotropy
 - Interface magnetic order
 - Curie temperature
 - Electron and spin transmission across interfaces
 - Exchange bias
 - Spin waves

Surface Magnetoelectric Effect on Fe (001)



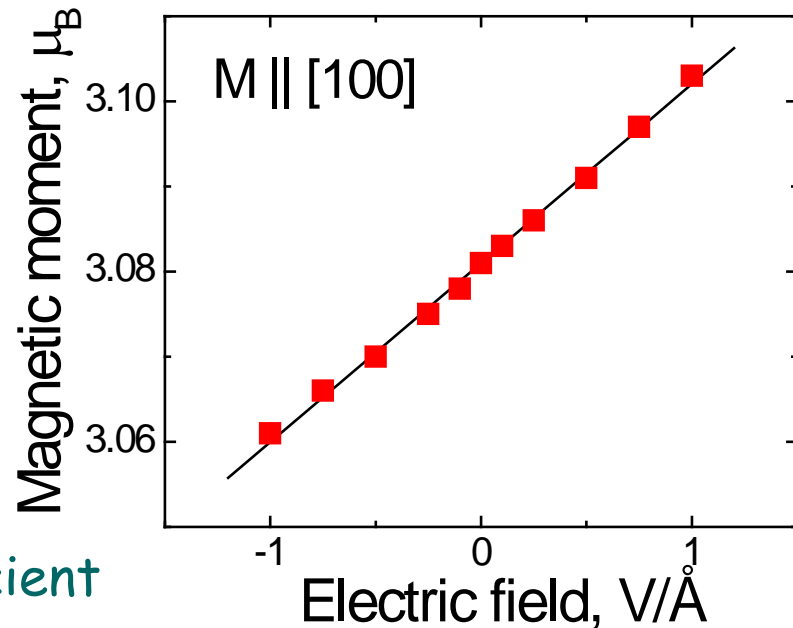
Duan et al, PRL 101, 137201 (2008)



- broken space inversion & time reversal symmetries

$$\mu_0 \Delta M = \alpha_s E$$

α_s - surface magnetoelectric coefficient



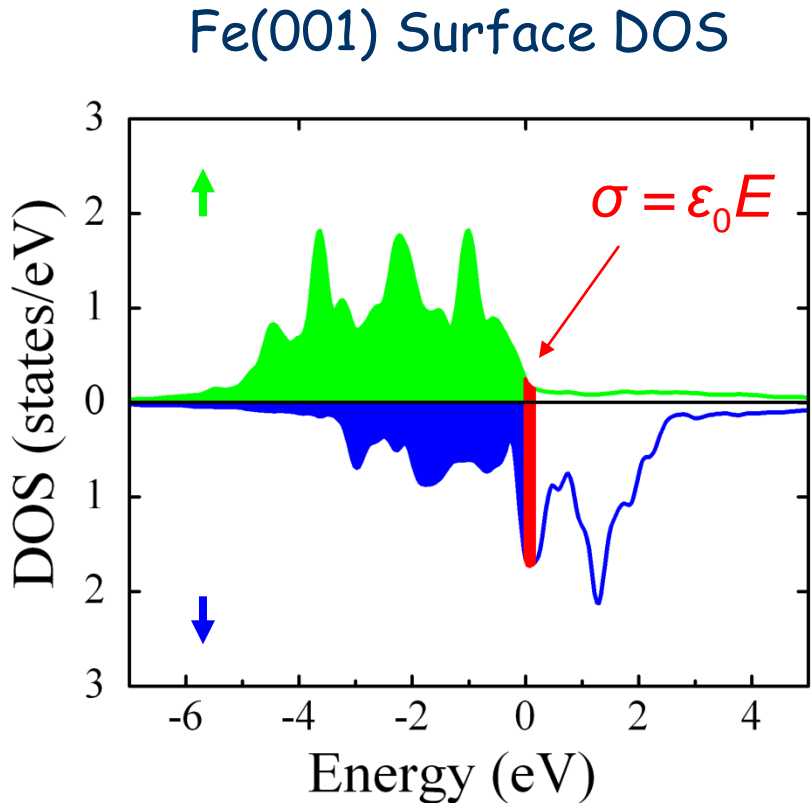
$$\alpha_s \approx 2.4 \times 10^{-14} \text{ G cm}^2/\text{V}$$

$$E = 1 \text{ V/nm} \rightarrow \Delta m \approx 2 \times 10^{-3} \mu_B \text{ per Fe}$$

- Electric field induces a surface magnetic moment
- Effect is small



Origin of Magnetoelectric Effect



$$\sigma = \sigma^{\uparrow} + \sigma^{\downarrow}$$

$$\sigma^{\uparrow} = \epsilon_0 E \frac{n^{\uparrow}}{n}; \quad \sigma^{\downarrow} = \epsilon_0 E \frac{n^{\downarrow}}{n}$$

$$\Delta M = \mu_B \frac{\sigma^{\uparrow} - \sigma^{\downarrow}}{e} = \frac{\epsilon_0 E \mu_B}{e} \frac{n^{\uparrow} - n^{\downarrow}}{n^{\uparrow} + n^{\downarrow}}$$

Magnetoelectric coefficient:

$$\alpha_s = \frac{\mu_B}{ec^2} \frac{n^{\uparrow} - n^{\downarrow}}{n^{\uparrow} + n^{\downarrow}} = \frac{\mu_B}{ec^2} P$$

$$\mu_0 \Delta M = \alpha_s E$$

- Fundamental limit for the linear ME effect
 - Universal constant for half-metals: $\alpha_s = \frac{\mu_B}{ec^2} \approx 6.44 \times 10^{-14} \text{ Gcm}^2 / \text{V}$
- Duan et al., PRB 79, R140403 (2009)

Ferroelectric Effect on Interface Magnetization



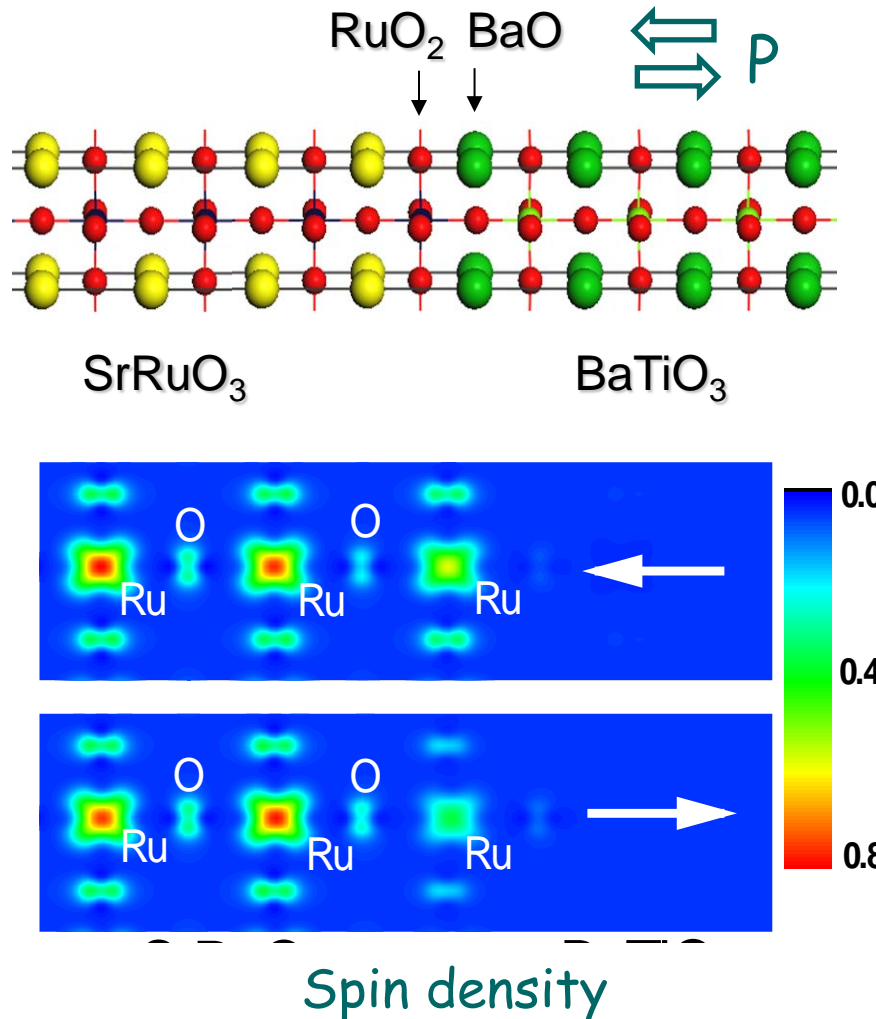
Niranjan et al, APL 95, 052501 (2009)



- Itinerant ferromagnet ($\sim 1 \mu_B/\text{f.u.}$)
- Curie temperature 160 K
- Perovskite structure
- Good lattice match to BaTiO_3
- Epitaxial strain to stabilize polarization (SrTiO_3 substrate)

$$\Delta m_{\text{Ru}} = 0.31 \mu_B$$

$$E_c \sim 0.1 \text{ V/nm}$$

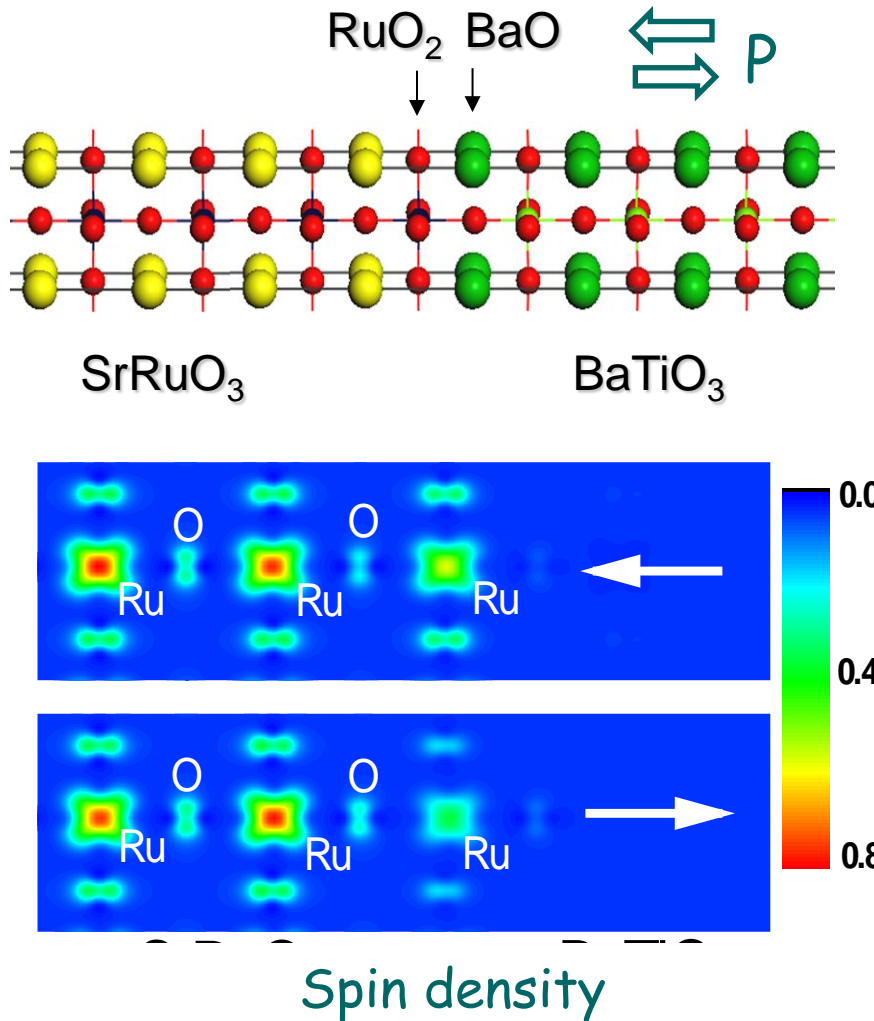
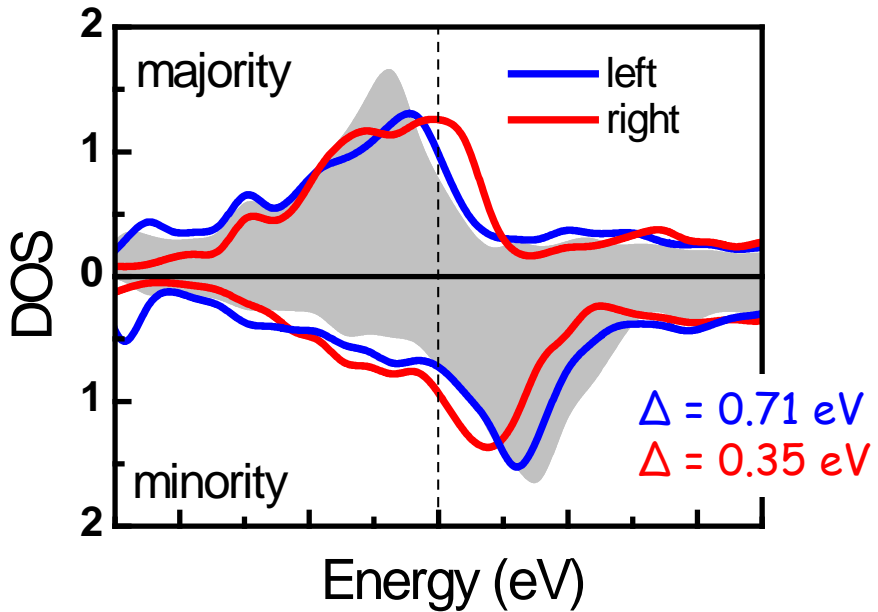


Ferroelectric Effect on Interface Magnetization



Niranjan et al, APL 95, 052501 (2009)

Spin resolved density of states



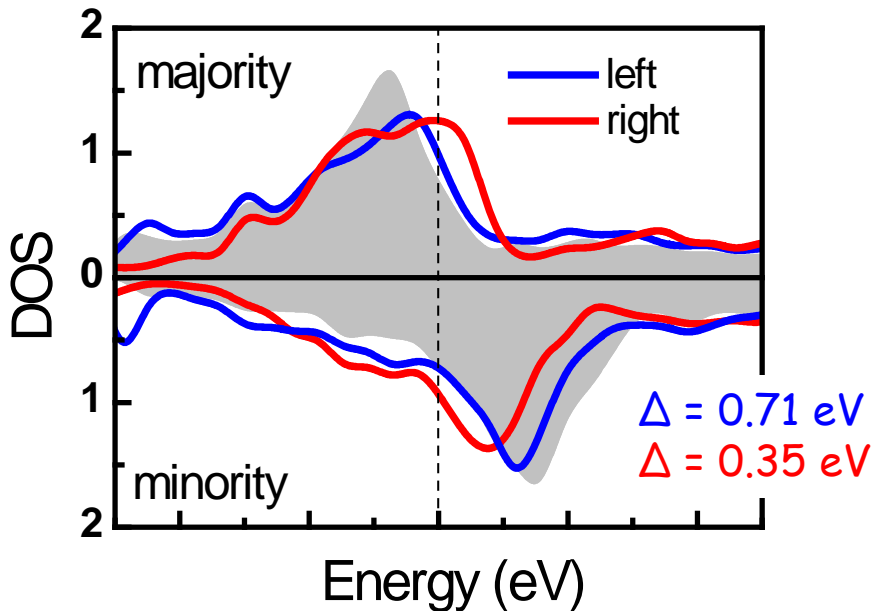
- Change in the exchange splitting at the interface

Ferroelectric Effect on Interface Magnetization



Niranjan et al, APL 95, 052501 (2009)

Spin resolved density of states



Stoner model
for itinerant magnetism:

$$\Delta = Im$$

I – Stoner exchange constant

$$\Delta = \frac{2\sqrt{\rho_F^2 I^2 - 1}}{|\rho'_F| I}$$

- Change in the exchange splitting at the interface

- Explains calculated change in exchange splitting with FE polarization reversal

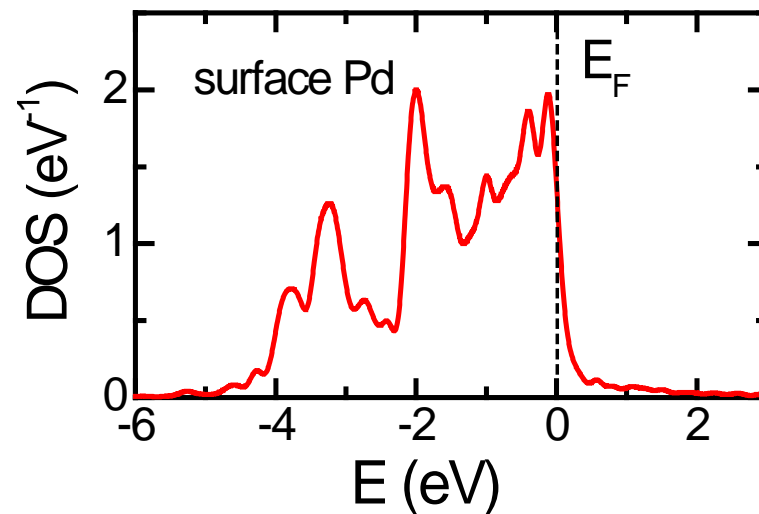
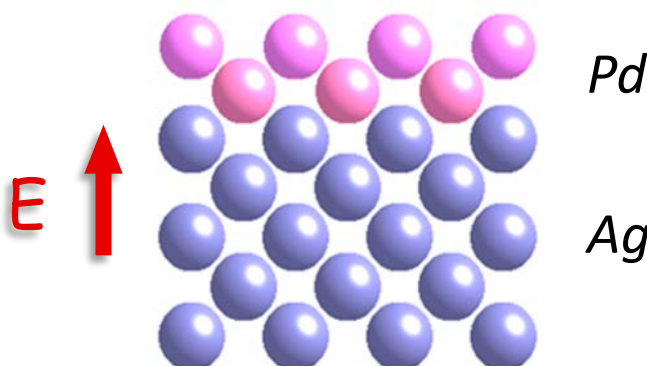
Inducing Magnetism on a Non-Magnetic Surface



Sun et al., PRB 81, 064413 (2010)

Stoner criterion for itinerant magnetism

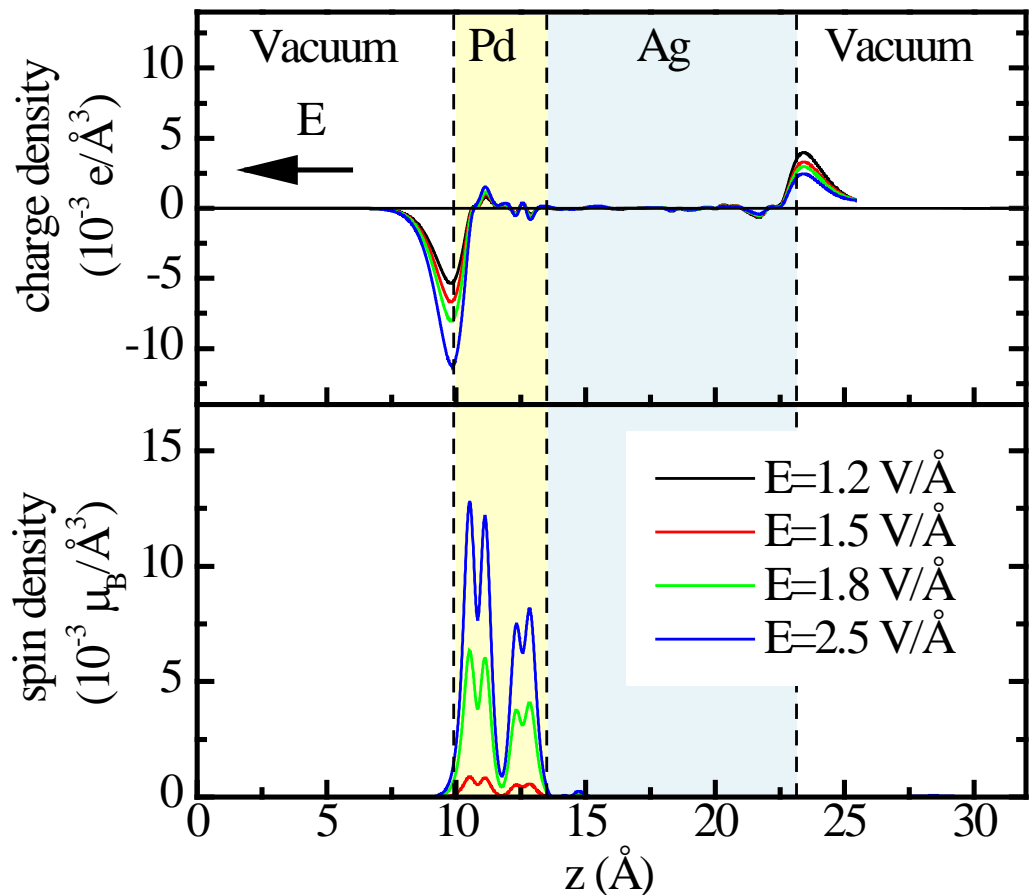
$$I\rho_F > 1$$



$$I \approx 0.65 \text{ eV}; \quad I\rho_F \approx 0.96$$

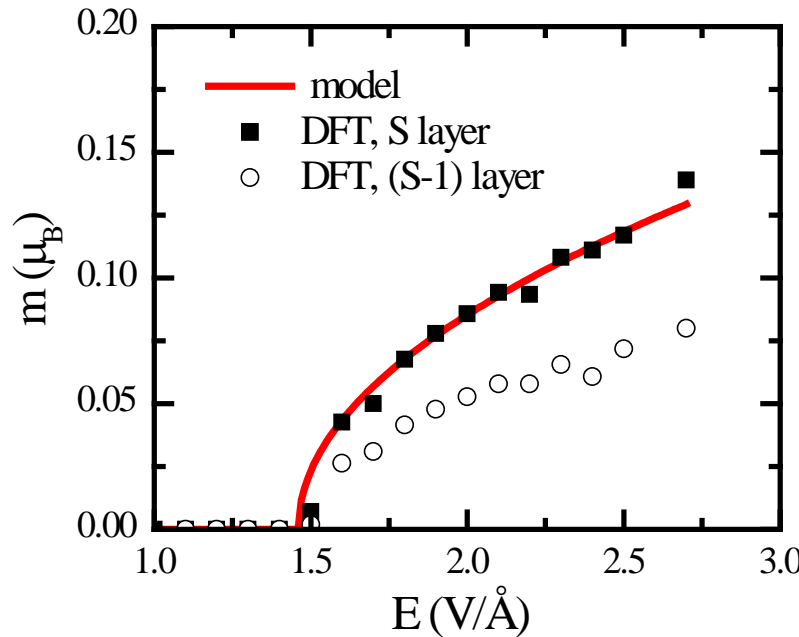
- Can we induce a surface magnetism by electric field ?

Electric-Field Induced Magnetism on a Pd (001) Surface



- Second-order phase transition
- Require very large electric fields which may be produced by an adjacent ferroelectric

Sun et al., PRB 81, 064413 (2010)



Linearized Stoner model:

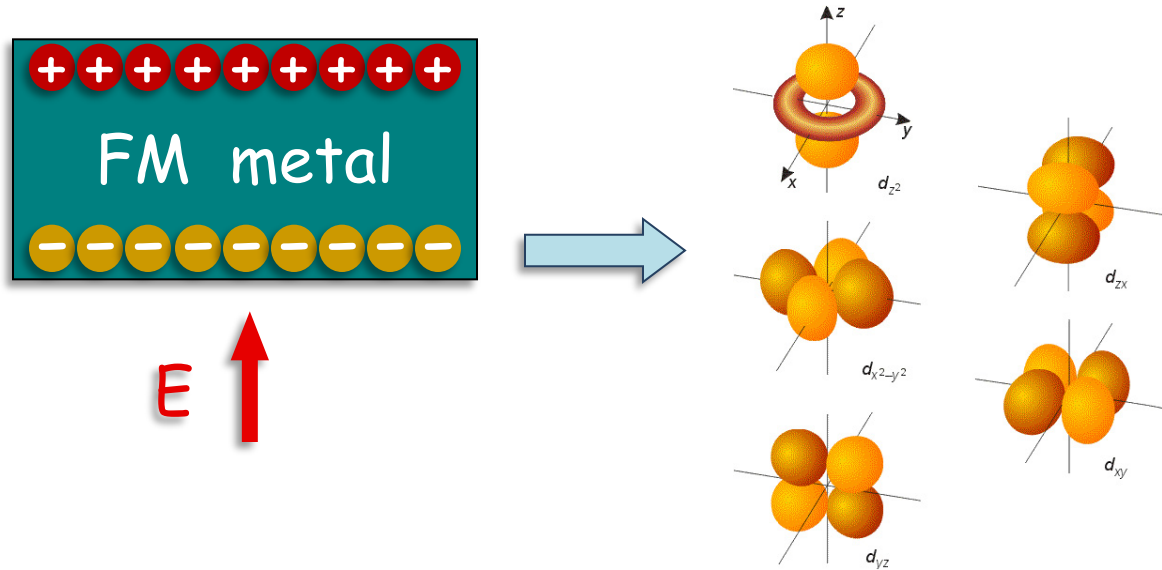
$$m(E) = \frac{2\sqrt{2\alpha\rho_F}}{I|\rho'_F|} \sqrt{E - E_c}$$

$$\rho_F(E) = \rho_F + \alpha E$$

Electric Field Effect on Magnetocrystalline Surface Anisotropy



- Electric field control of magnetization orientation



- Screening charge induced by electric field
 - Change in relative population of d-orbitals at the surface
 - Change in surface magnetocrystalline anisotropy (MCA)

$$\Delta K = \beta_s E$$

β_s - VCMA coefficient

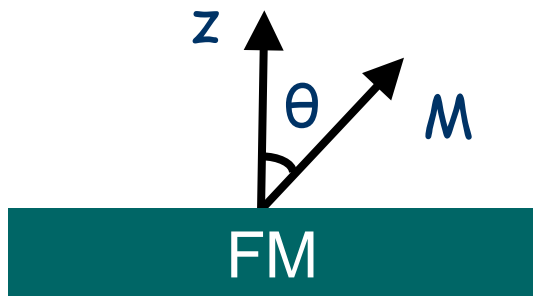


Magnetic Anisotropy

- Bulk magnetocrystalline anisotropy (MCA)
- Surface (interface) MCA
- Shape anisotropy

MCA energy determined by spin-orbit interaction:

$$H = \xi \mathbf{L} \cdot \mathbf{S}$$



In thin films:

$$E_{\text{shape}} \approx \mu_0 M^2 \cos^2 \theta \quad - \text{volume}$$

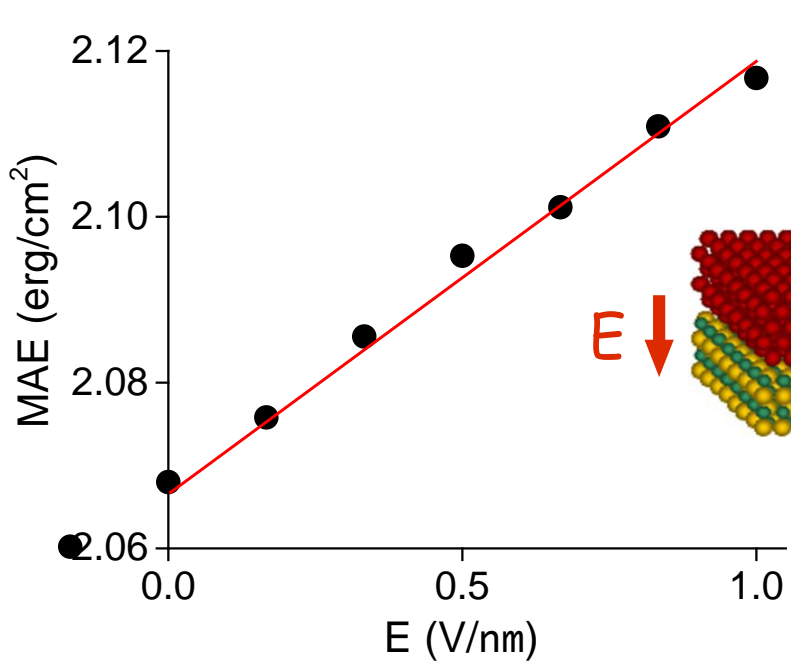
$$E_{\text{surface}} \approx -K_S \cos^2 \theta \quad - \text{surface}$$

$$K \propto \sum_{o,u} \frac{\left| \langle o | L_z | u \rangle \right|^2 - \left| \langle o | L_x | u \rangle \right|^2}{\varepsilon_u - \varepsilon_o}$$

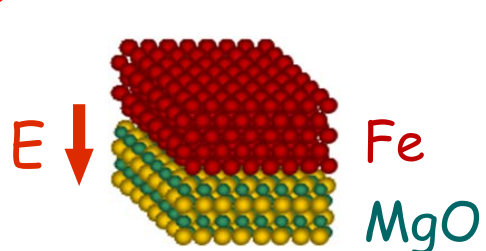
within 2nd order perturbation theory

- sensitive to orbital population

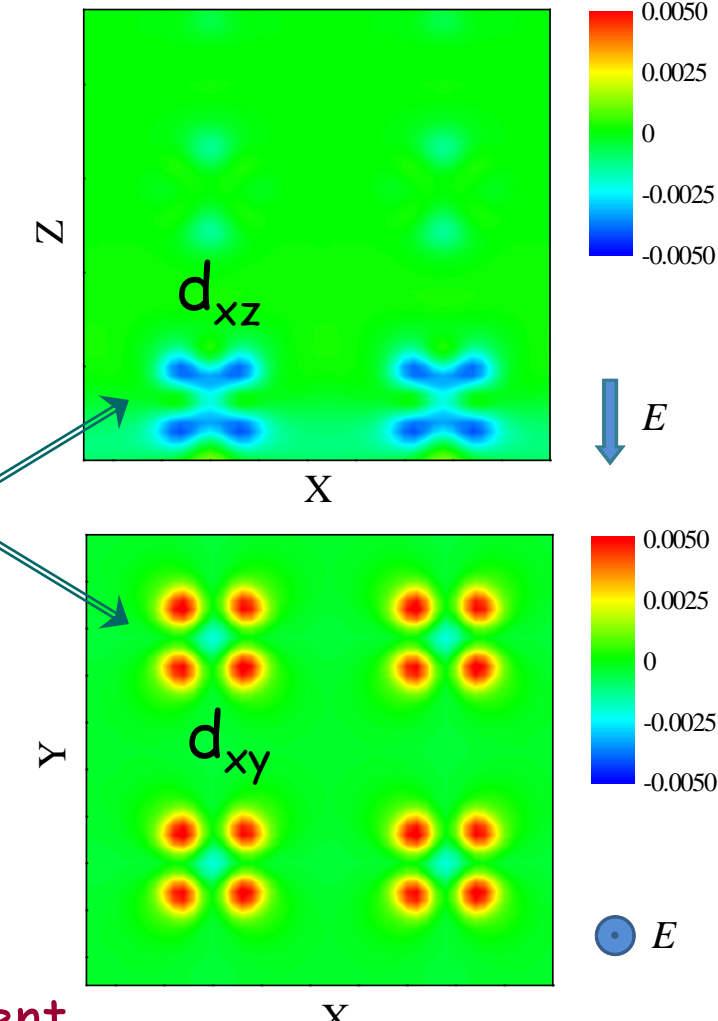
Fe/MgO(100) Interface



Niranjan et al., APL 96, 222504 (2010)



Interface
Fe atoms

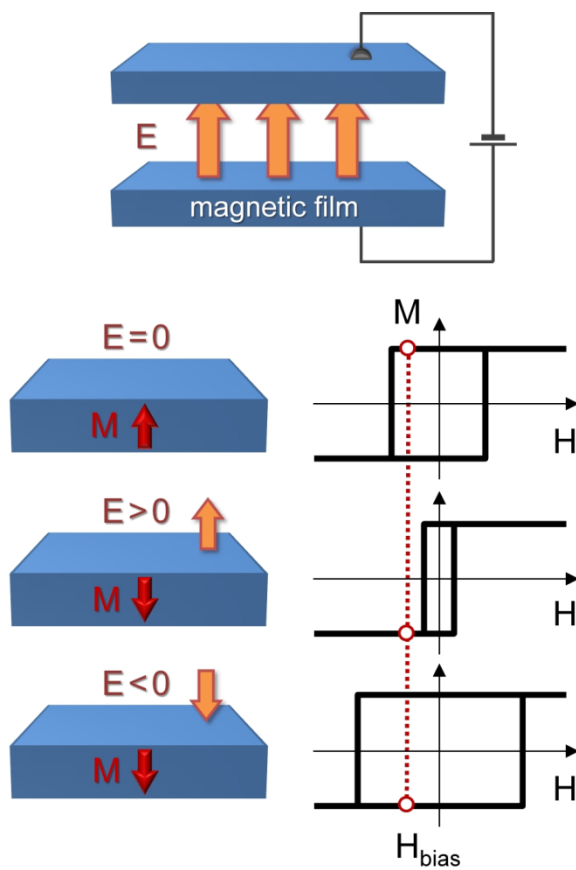


- Large perpendicular magnetic anisotropy (PMA): $K \sim 2 \text{ erg/cm}^2$
- Increases with field away from interface
- Effect due to change in occupation of Fe-3d orbitals ($d_{xz}, d_{yz} \rightarrow d_{xy}$)

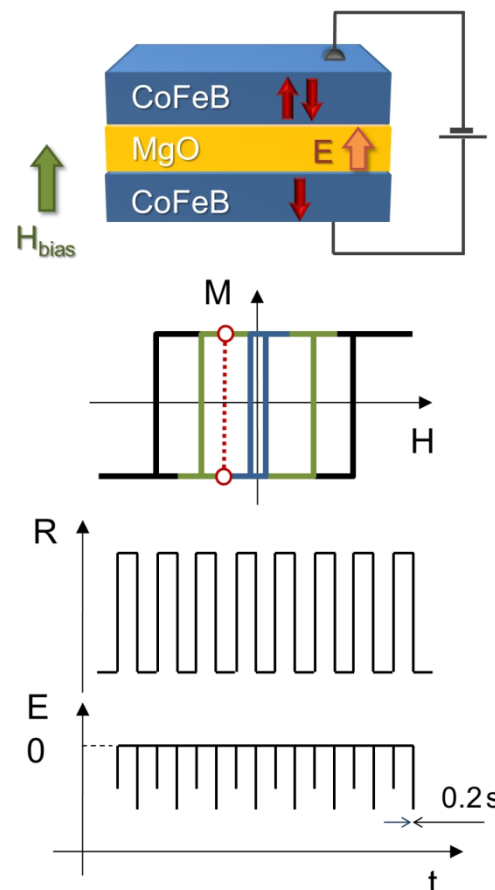
$\beta_s \approx 0.05 \text{ pJ/Vm}$ - consistent with experiment

Toggle Switching of Magnetization

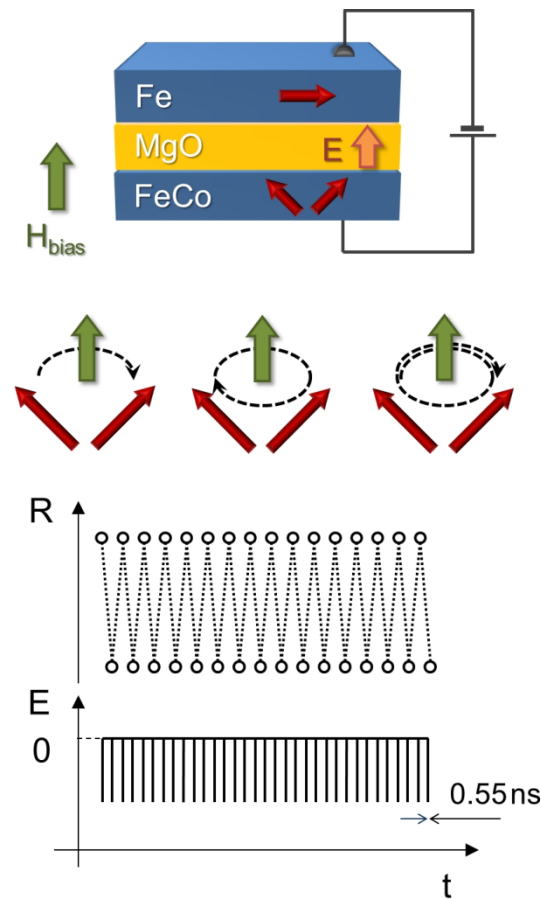
Tsybala,
Nat. Mater. 11, 12 (2012)



Wang et al.,
Nat. Mater. 11, 64 (2012)



Shiota et al.,
Nat. Mater. 11, 39 (2012)



□ Significant interest from industry

Ferroelectric Control of Magnetic Interface Anisotropy



Lukashev et al., JPCM 24, 226003 (2012)

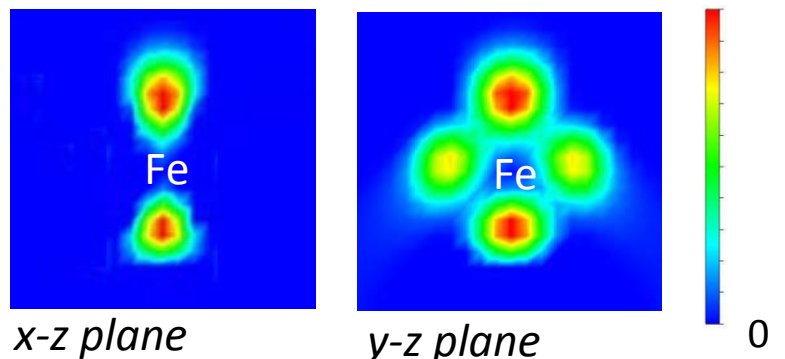
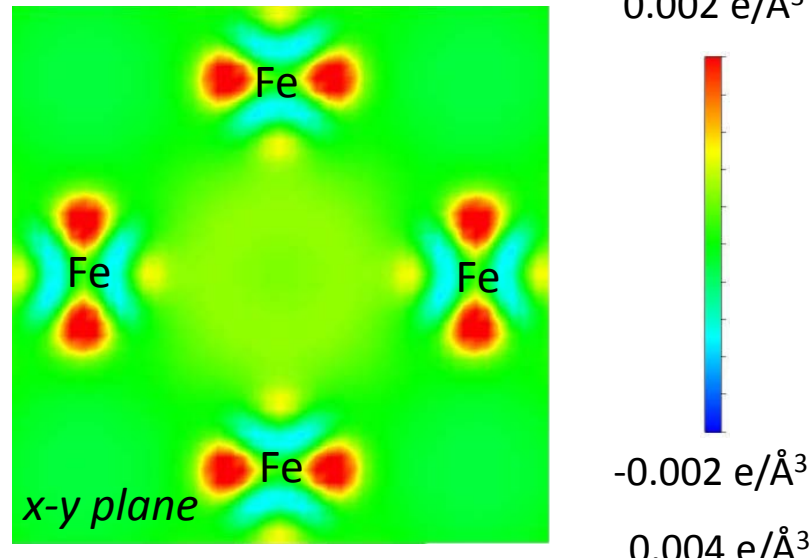


$$K \approx 1.3 \text{ erg/cm}^2 \quad K \approx 1.0 \text{ erg/cm}^2$$

- Large perpendicular anisotropy
- Large change with polarization switching
- Effect due to the relative change in 3d orbitals occupation
- Consistent with Fe/MgO

$$E_c \sim 0.1 \text{ V/nm} \Rightarrow \beta_s \sim 3 \text{ pJ/Vm}$$

Induced charge density

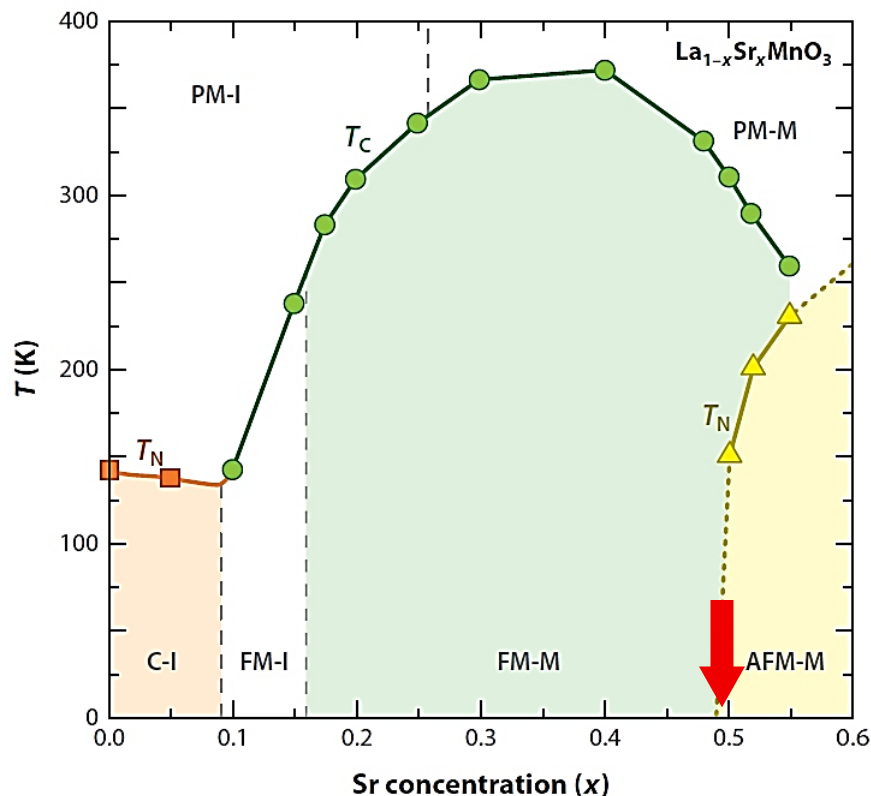


- VCMA effect enhanced by two orders in magnitude!

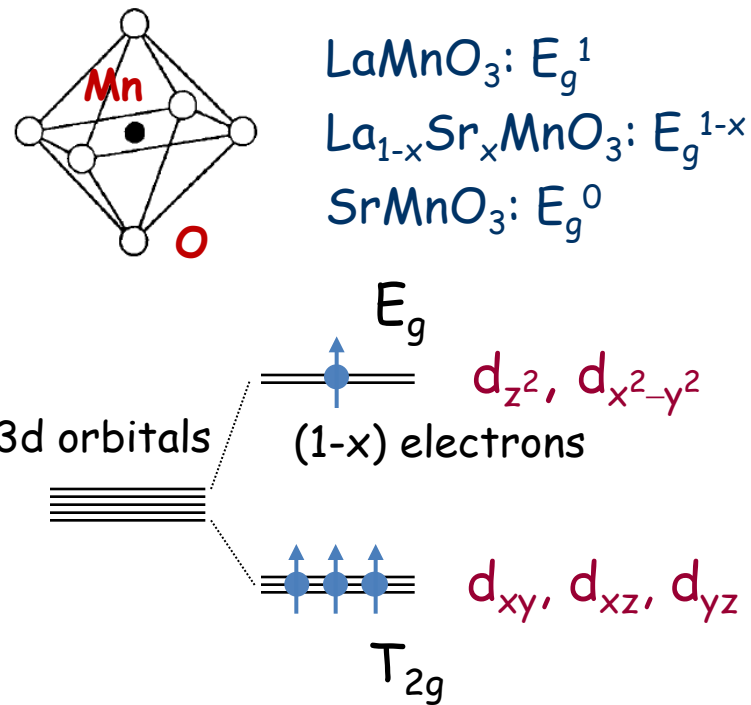
Electrostatic Doping of Magnetic Perovskites: $\text{La}_{1-x}\text{A}_x\text{MnO}_3$

- Magnetic perovskites: $\text{La}_{1-x}\text{A}_x\text{MnO}_3$ ($\text{A}^{2+} = \text{Ca}, \text{Sr}, \text{Ba}$)

$\text{La}_{1-x}\text{Sr}_x\text{MnO}_3$



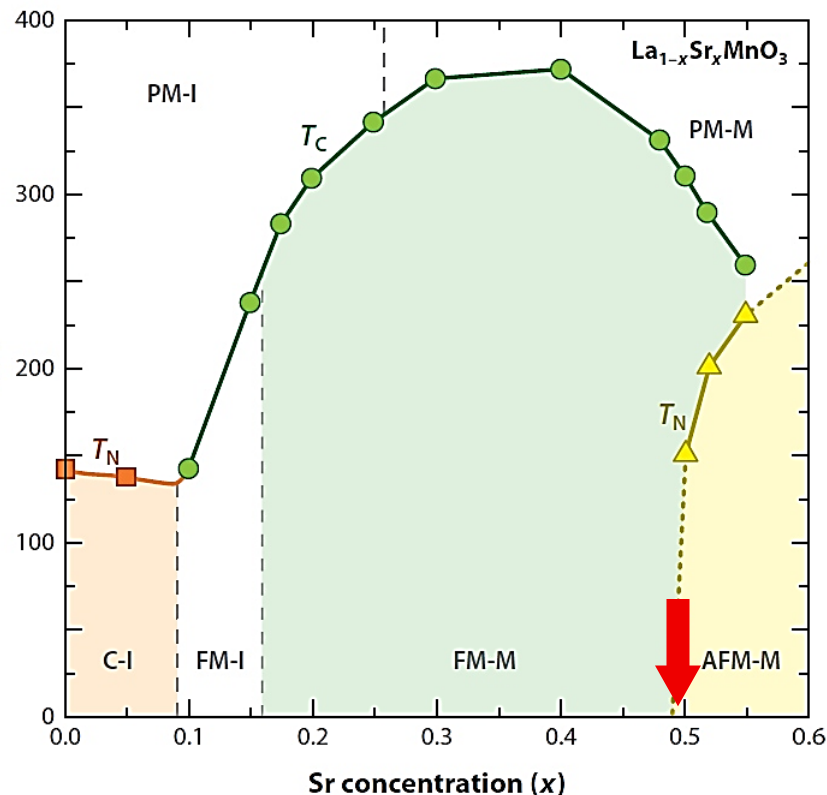
Hole doping of LaMnO_3 :



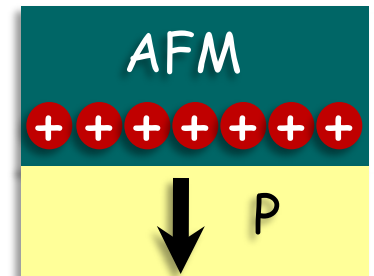
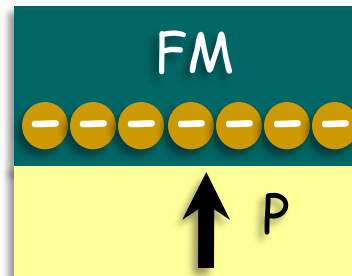
- Transition from FM to AFM order near $x \sim 0.5$

Electrostatic Doping of Magnetic Perovskites: $\text{La}_{1-x}\text{A}_x\text{MnO}_3$

- Magnetic perovskites: $\text{La}_{1-x}\text{A}_x\text{MnO}_3$ ($\text{A}^{2+} = \text{Ca}, \text{Sr}, \text{Ba}$)



Changing magnetic order by "electrostatic doping" at an interface with a ferroelectric?

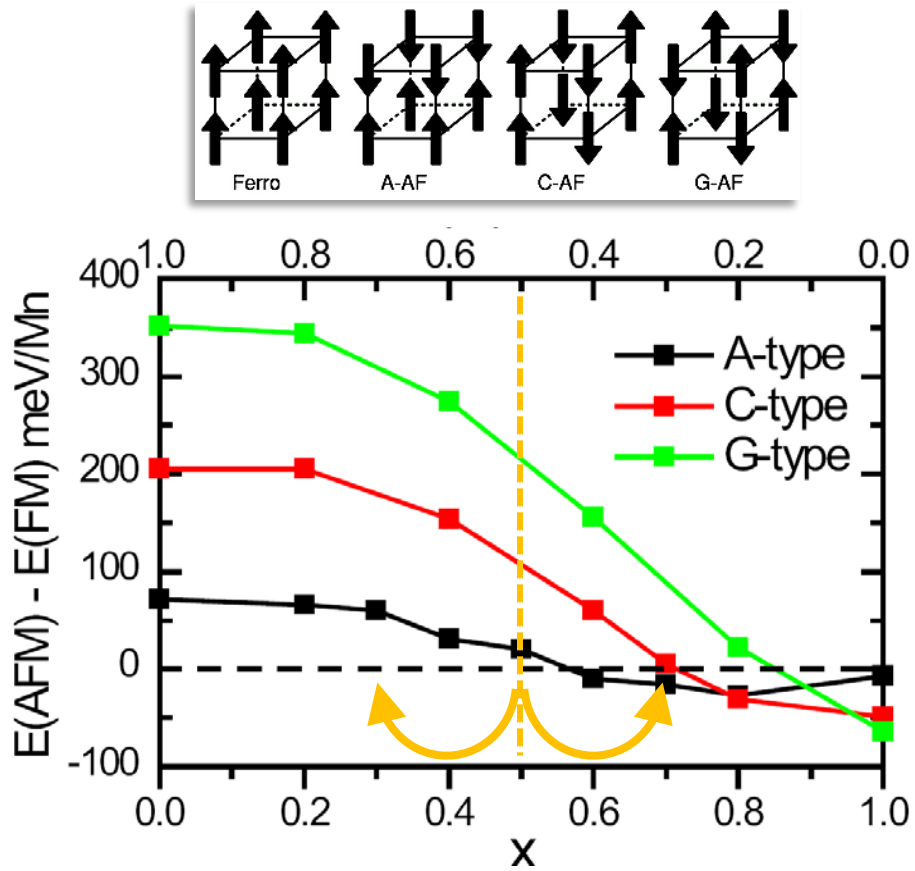
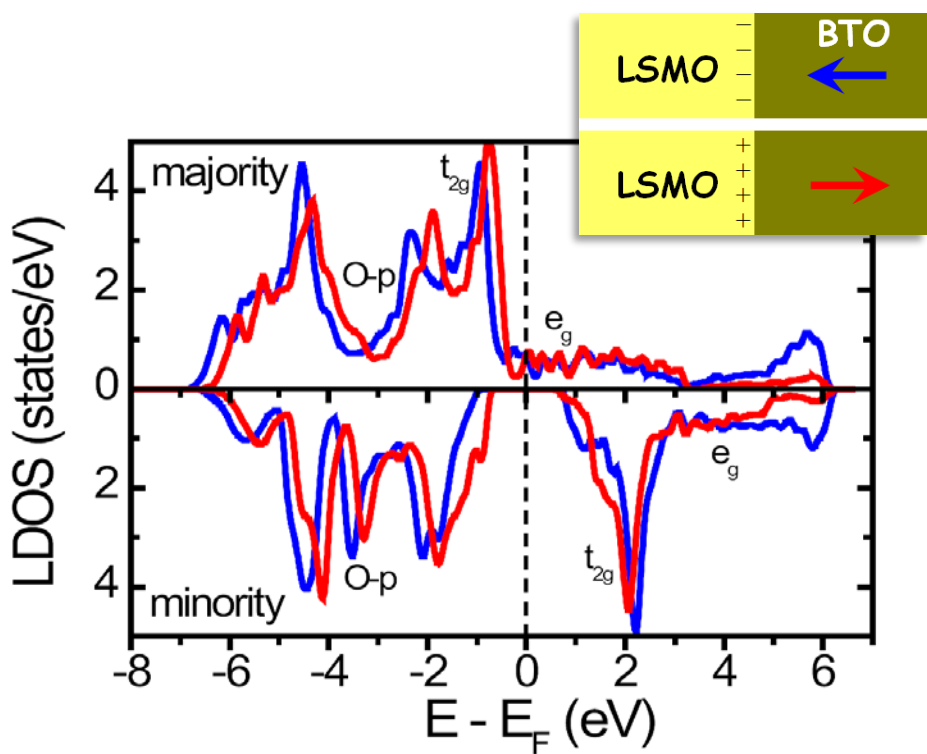


- Transition from FM to AFM order near $x \sim 0.5$

Interface Electronic Structure of $\text{La}_{0.5}\text{Sr}_{0.5}\text{MnO}_3$



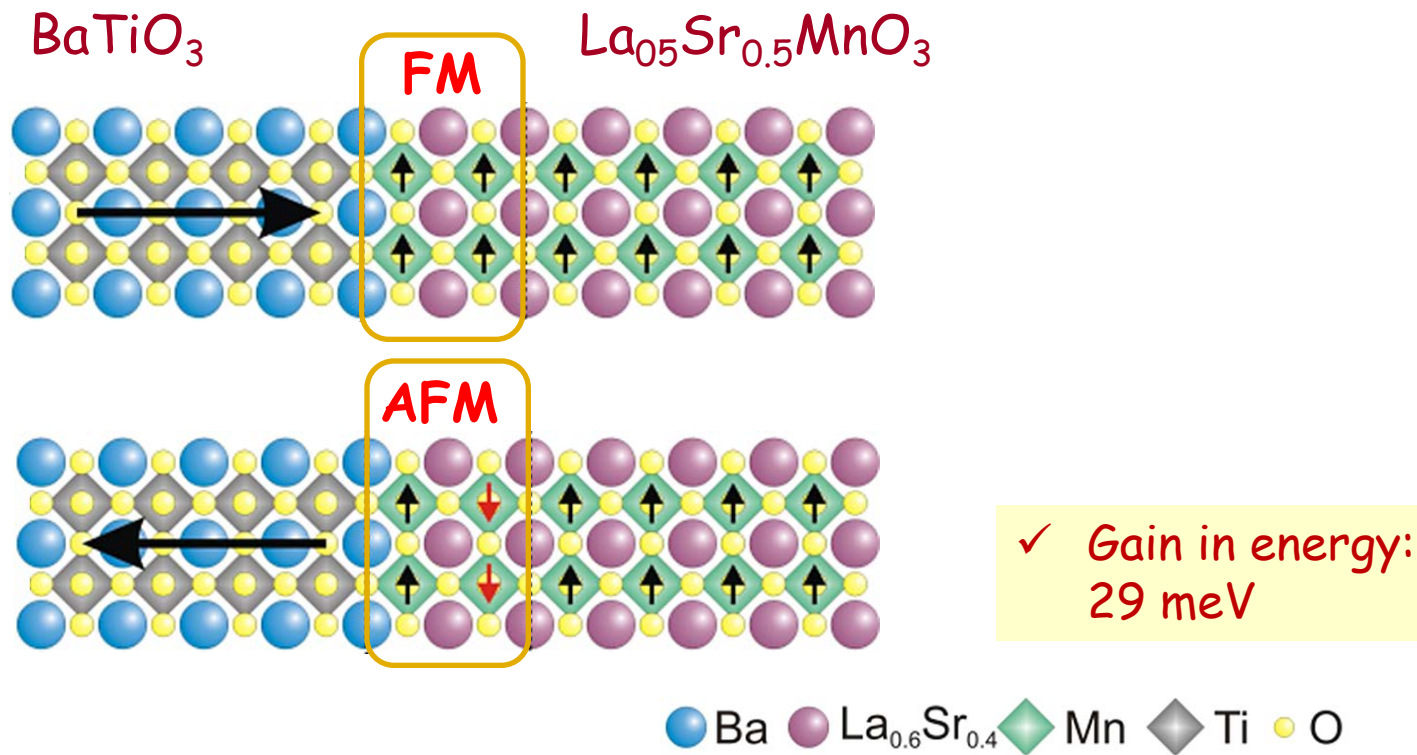
Burton et al., PRB 80, 174406 (2009)



- Accumulation or depletion of electronic charge controls majority-spin e_g state population and thus magnetic order

Interface Magnetic Reconstruction

Burton et al., PRB 80, 174406 (2009)

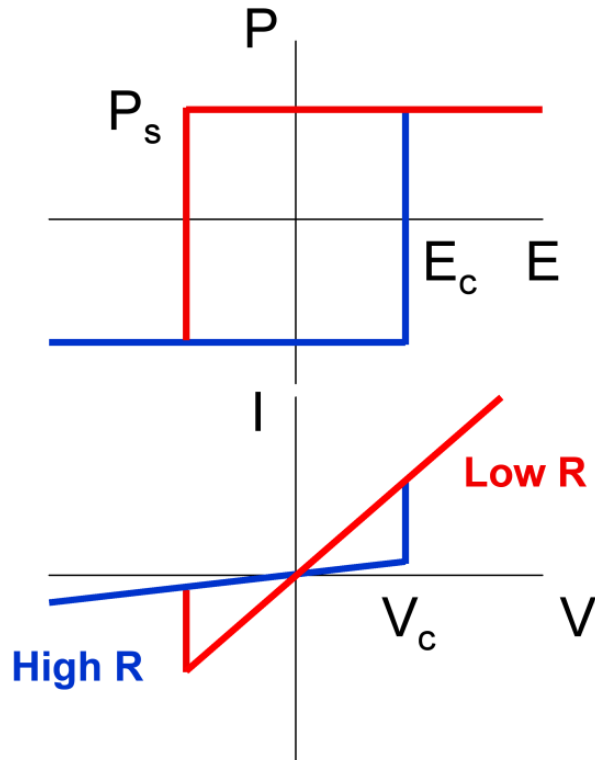
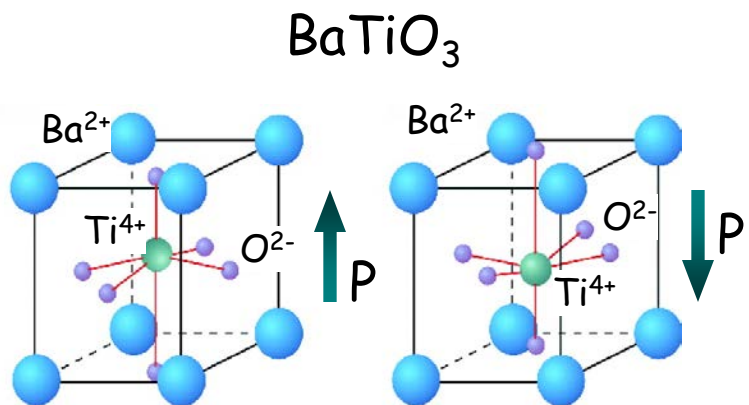


- Change in the local magnetic order from FM to AFM induced by ferroelectric polarization reversal



Ferroelectric Tunnel Junction (FTJ)

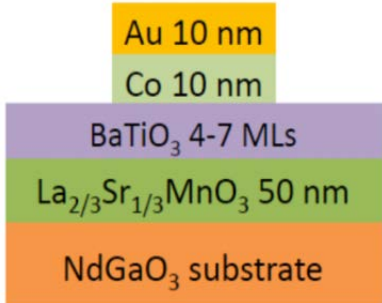
Tsymbal et al., Science 313, 181 (2006);
MRS Bulletin 37, 138 (2012)



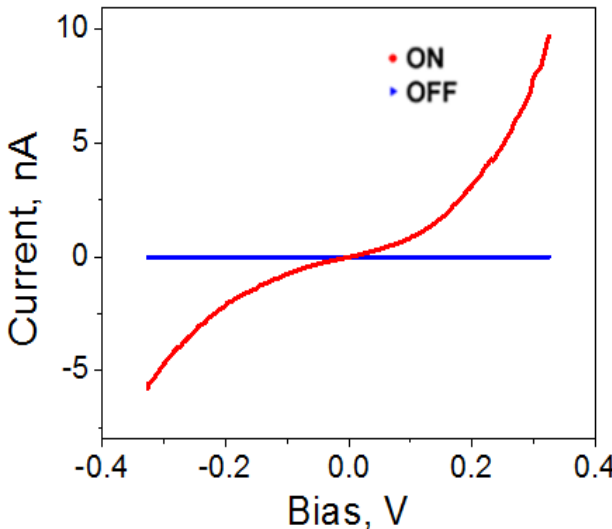
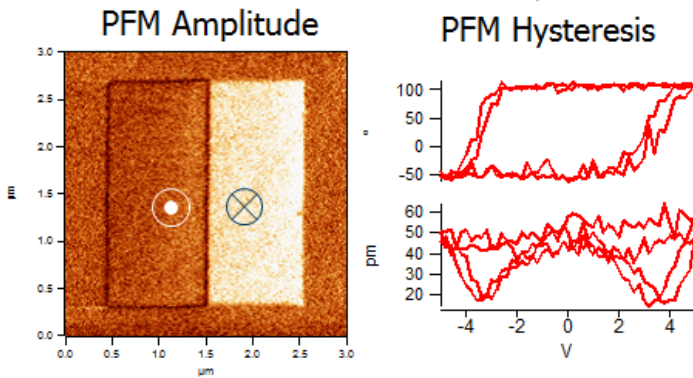
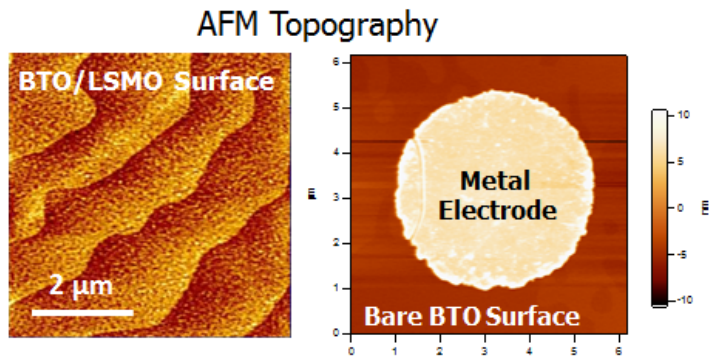
- Tunneling Electroresistance (TER) effect:
resistive switching of FTJ at coercive electric field



Reliable FTJ Devices



Kim et al.,
Nano Lett. 12, 5697 (2012)



- ✓ FTJs with ON/OFF resistance ratio exceeding 10^3 at room temperature



Multiferroic Tunnel Junction (MFTJ)

Zhuravlev et al, APL 87, 222114 (2005); PRB 81, 104419 (2010)

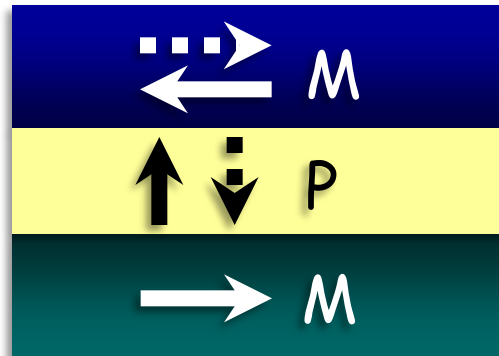
- Magnetic tunnel junction with a ferroelectric barrier

$$\text{MFTJ} = \text{MTJ} + \text{FTJ}$$

Ferromagnet

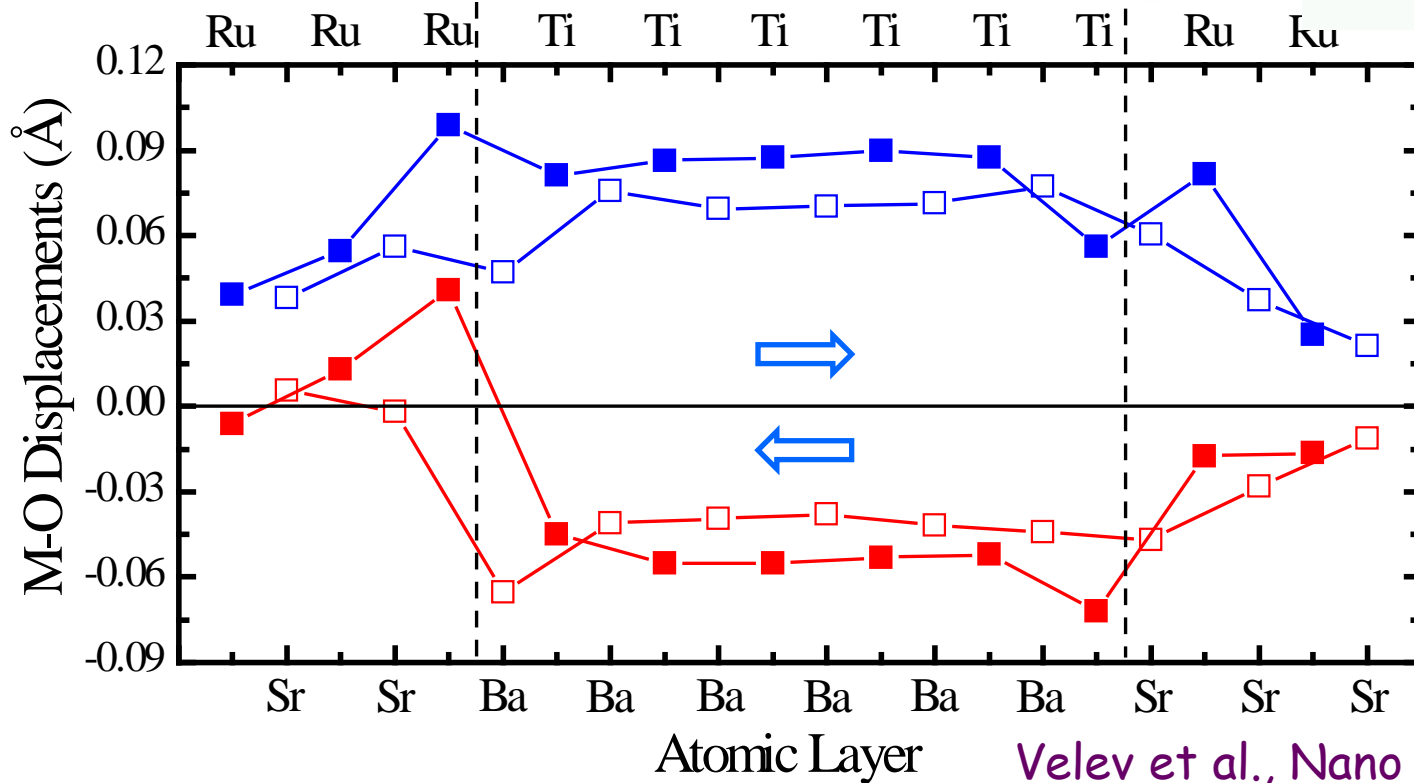
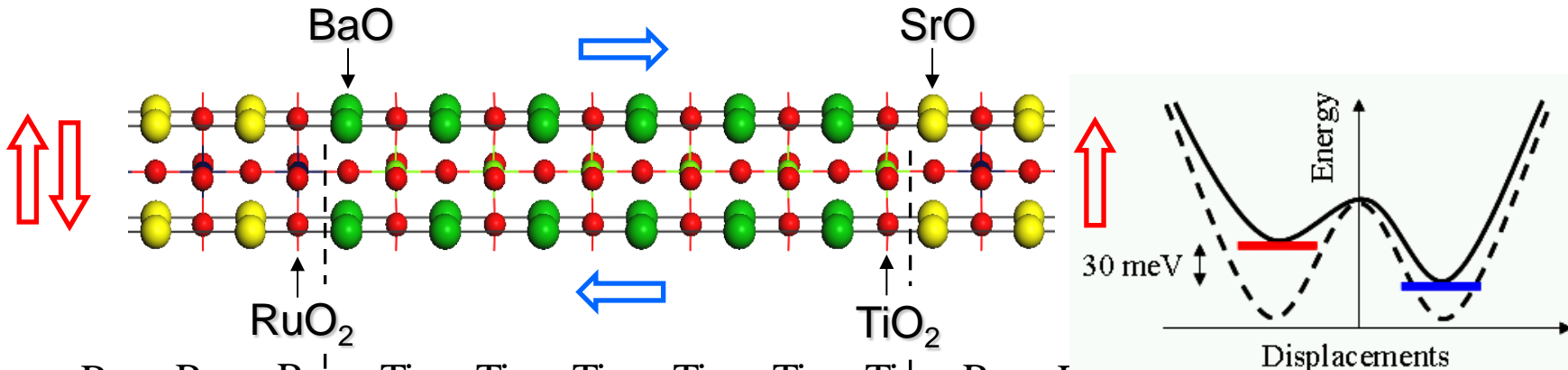
Ferroelectric

Ferromagnet



- MFTJ combines TMR with TER making a four-state resistive device
- Effect of ferroelectric polarization on transport spin polarization
- Multifunctional properties

$\text{SrRuO}_3/\text{BaTiO}_3/\text{SrRuO}_3$ Multiferroic Tunnel Junction (MFTJ)

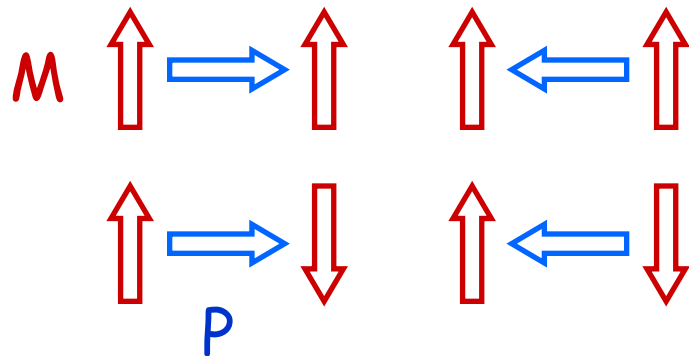


Velev et al., Nano Lett. 9, 427 (2009)



Co-existence of TER and TMR

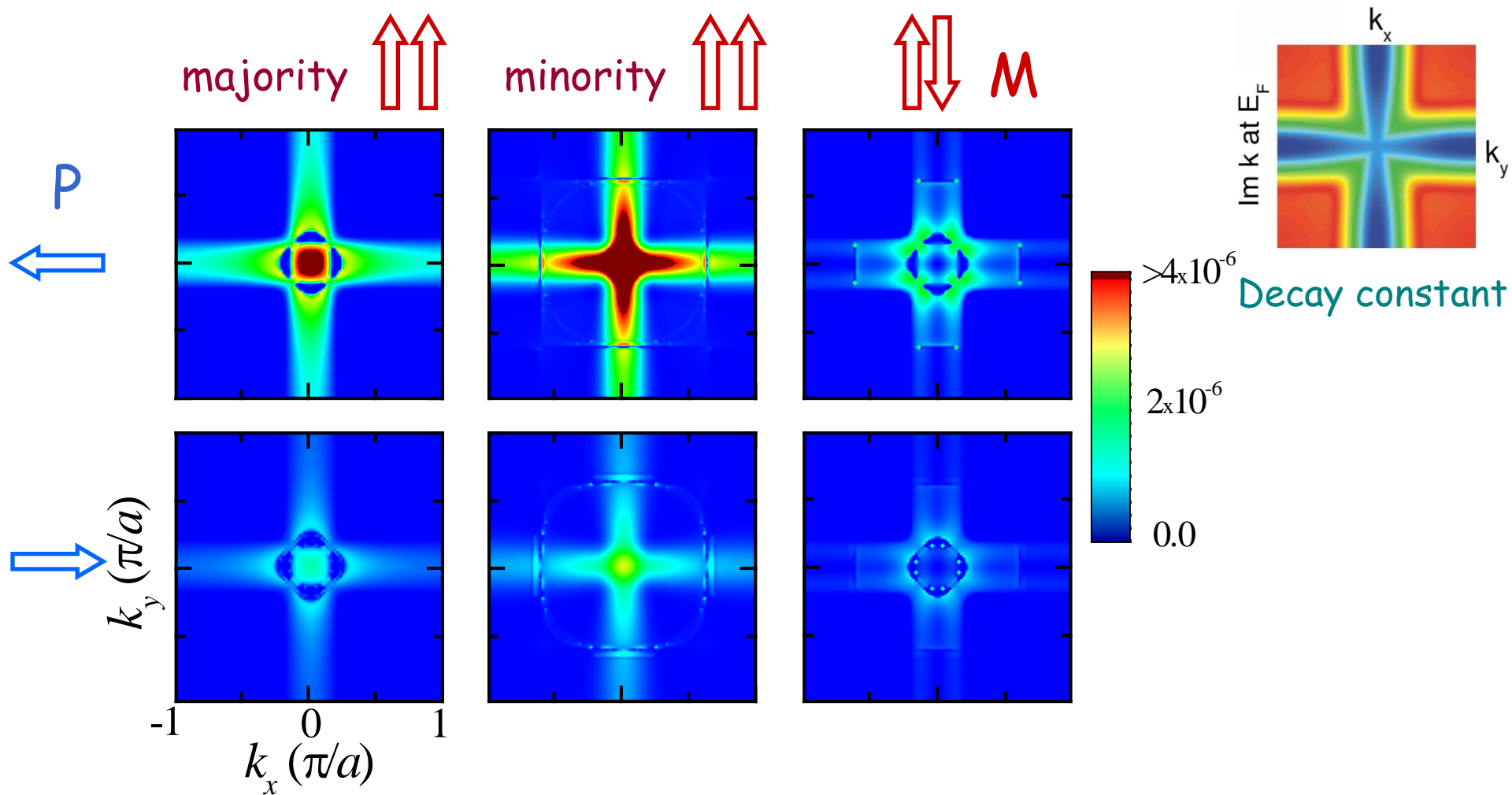
Velev et al., Nano Lett. 9, 427 (2009)



Four conductance states in $\text{SrRuO}_3/\text{BaTiO}_3/\text{SrRuO}_3$ MFTJ

G ($10^{-7}e^2/h$)	$\uparrow\uparrow$	$\uparrow\downarrow$	TMR (%)
→	3.76	0.83	350
←	11.82	1.69	590
TER (%)	210	100	

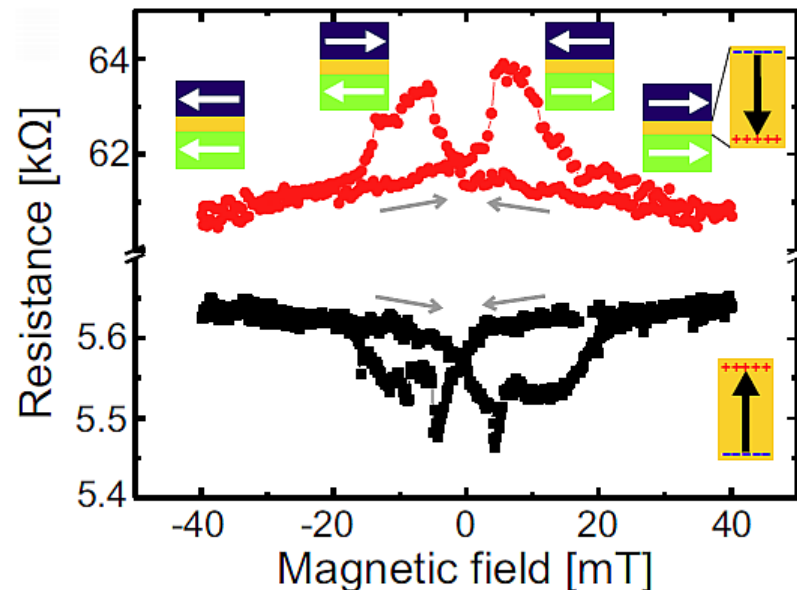
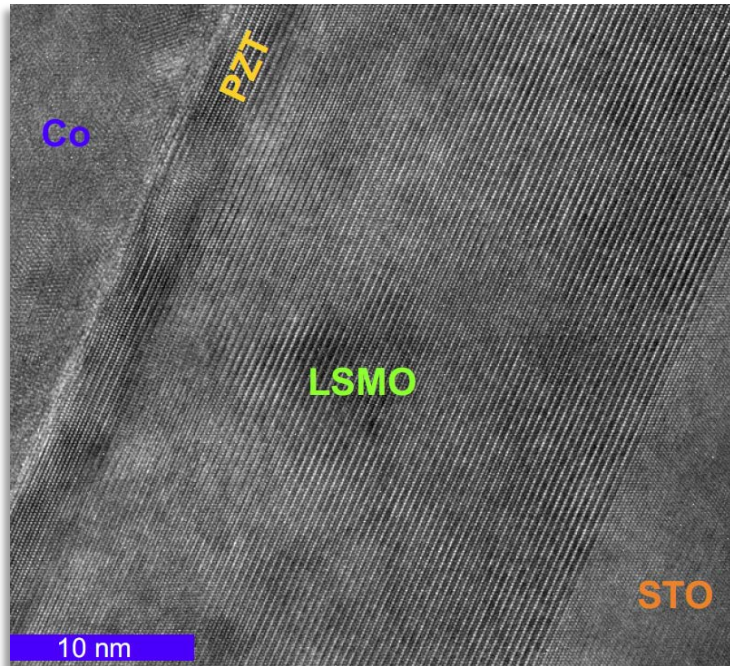
$K_{||}$ -resolved Transmission



- TMR - selection rules for electronic transmission
- TER - attenuation constant in the barrier

Ferroelectric Control of Spin Polarization

Pantel et al., Nature Mater. 11, 289 (2010)

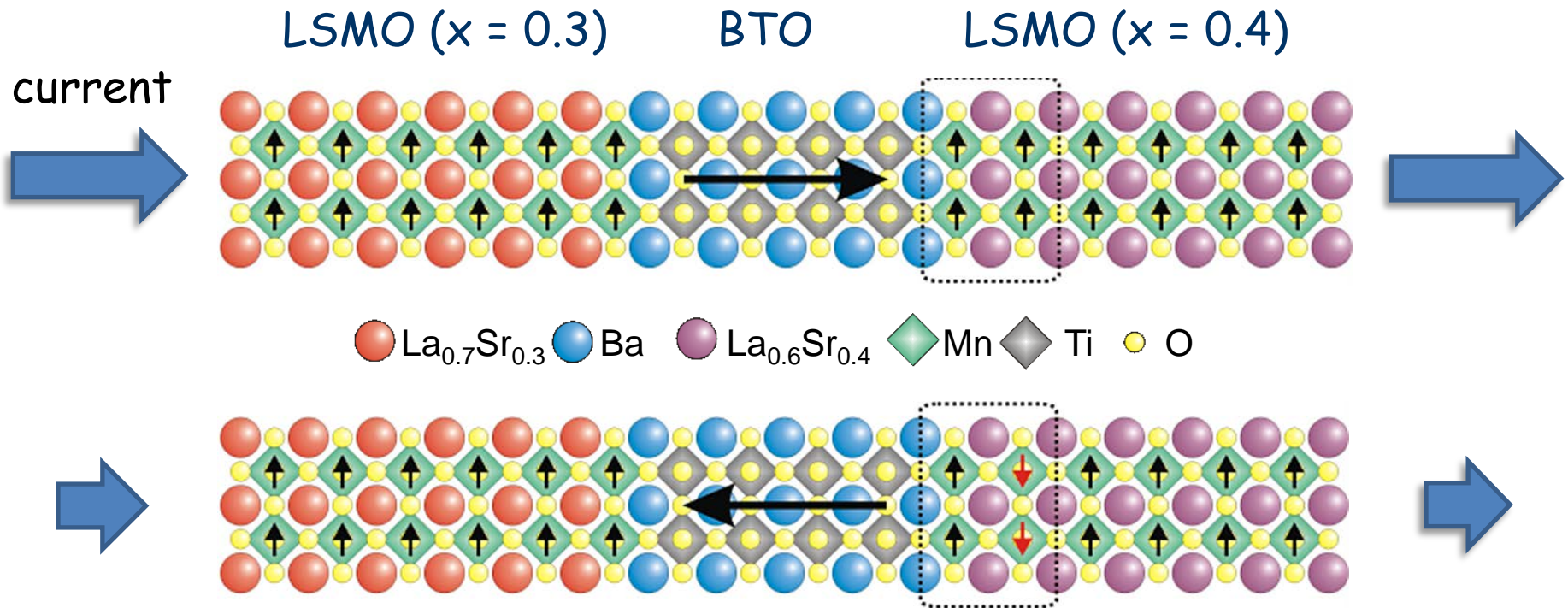


- Coexistence of TMR and TER
- Change of TMR sign with ferroelectric polarization reversal

Magnetoelectrically Driven TER Effect



Burton et al., PRL 106, 157203 (2011)

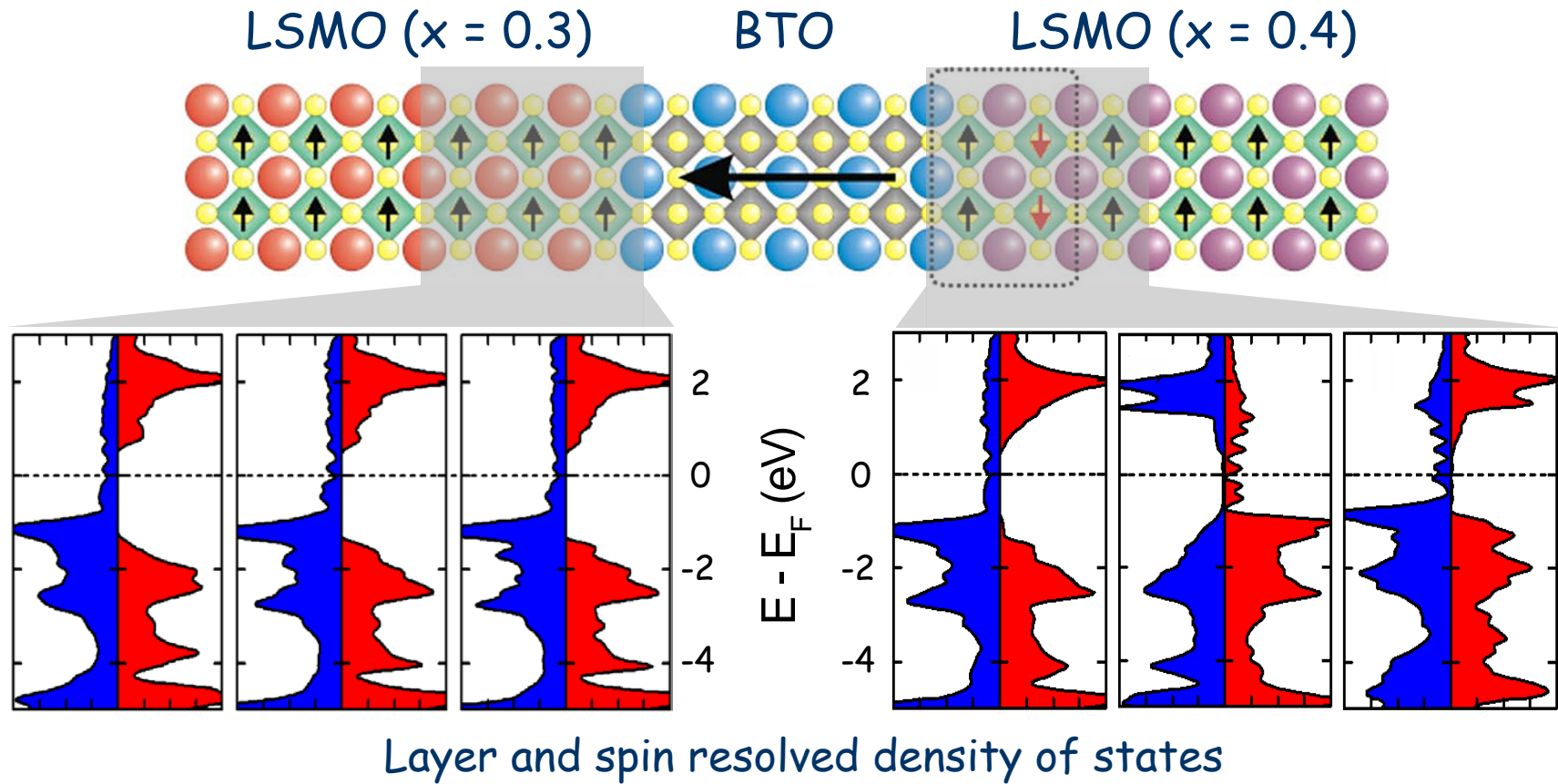


- More than 20 fold change in resistance !

Electrically-Controlled Atomic Spin Valve



Burton et al., PRL 106, 157203 (2011)



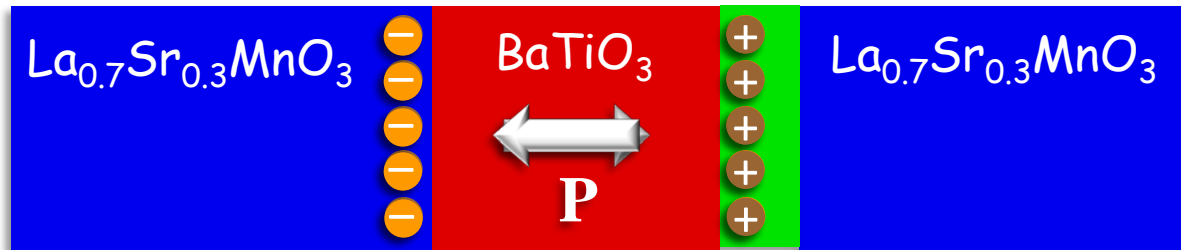
- Polarization driven magnetic moment reversal acts as a spin valve enhancing dramatically resistance for antiparallel state



Experiments

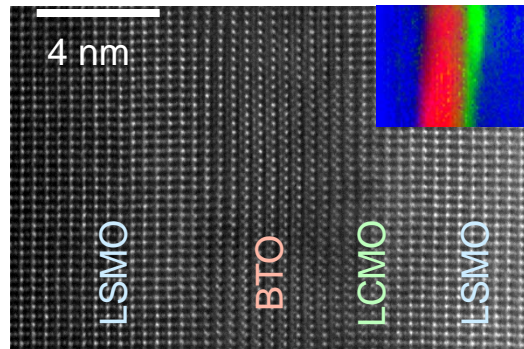
Yin et al., Nature Mater. 12, 397 (2013)

AFFMIMulator

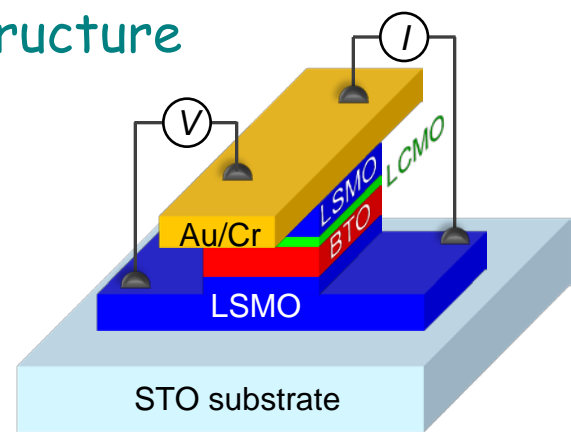


$\text{La}_{0.5}\text{Ca}_{0.5}\text{MnO}_3$
 $\sim 1\text{nm}$

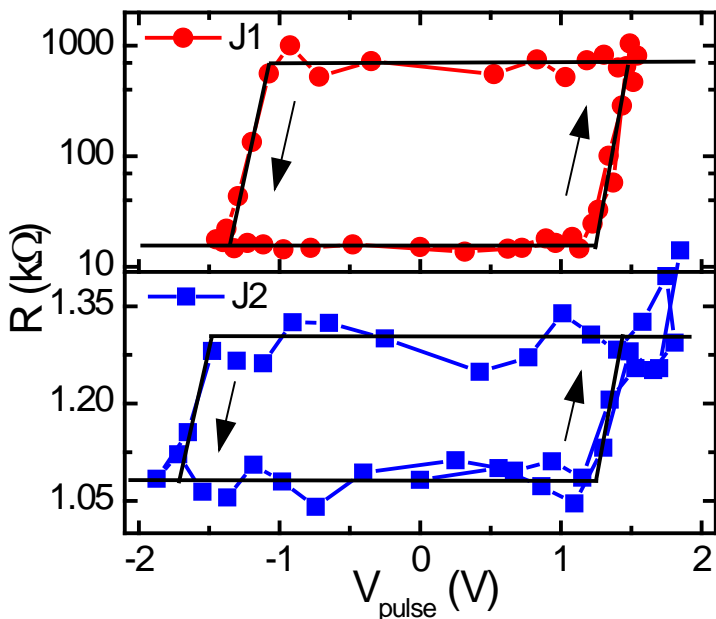
HRTEM & EELS



Device structure

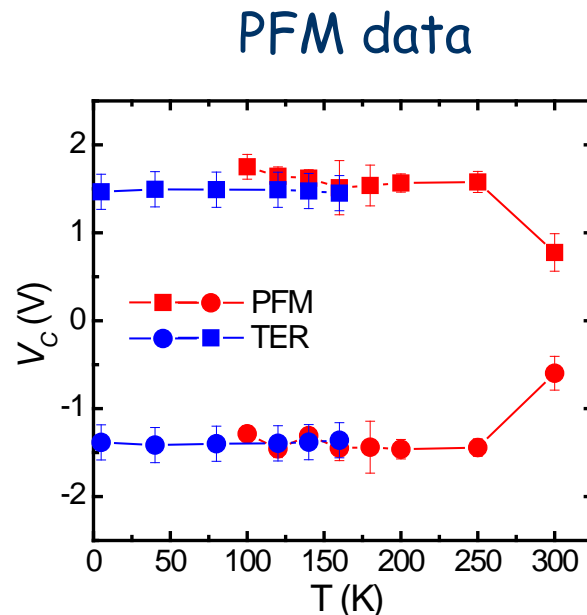
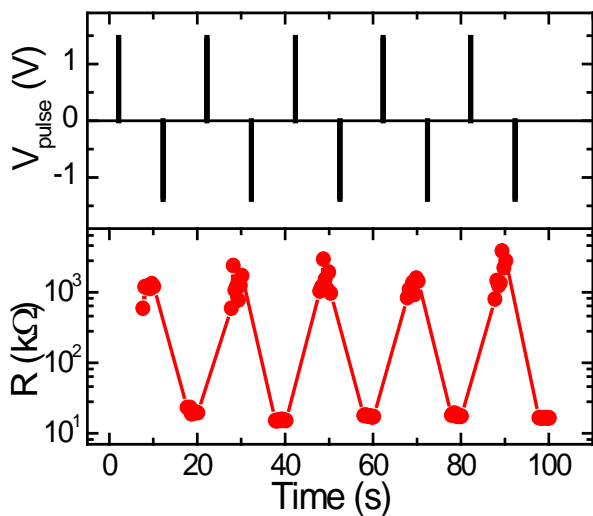


Experimental Result: ~10,000% TER



with LCMO
interlayer
TER $\sim 10,000\%$

without LCMO
interlayer
TER $\sim 40\%$

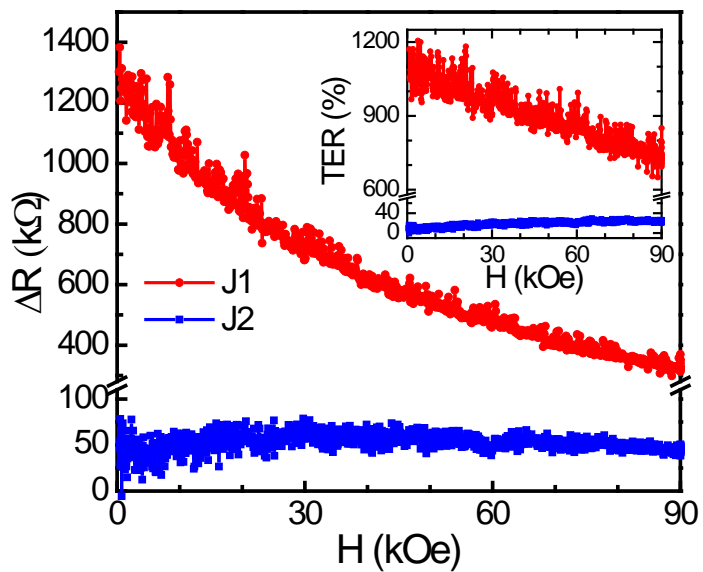


- TER associated with FE polarization switching
- Effect is reversed when LCMO is deposited on bottom interface
- Reproducible switching behavior

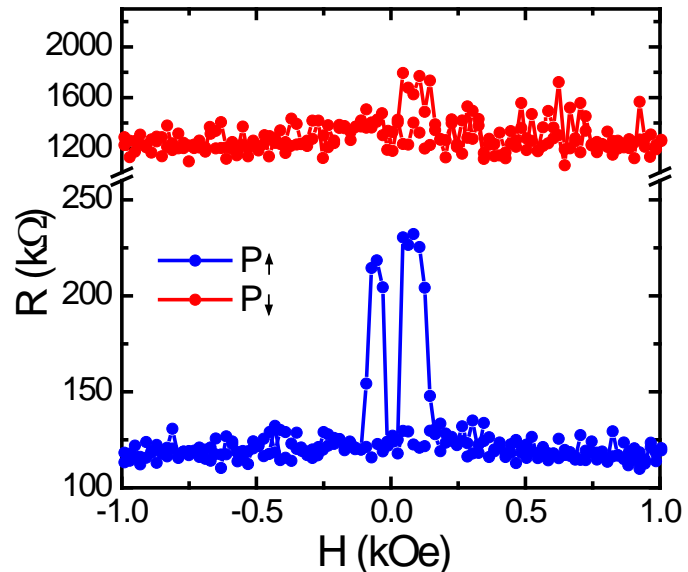
Magnetoresistance

Yin et al., Nature Mater. 12, 397 (2013)

High field data



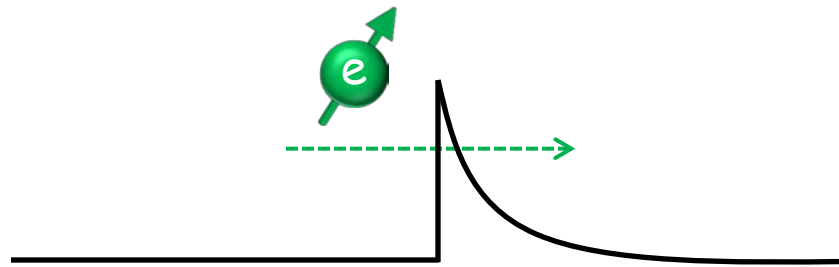
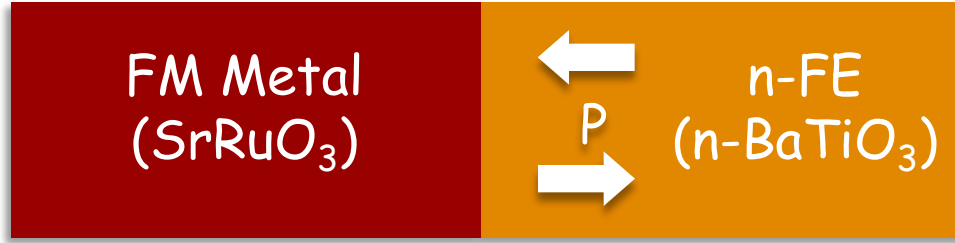
TMR



- Consistent with the magnetic reconstruction mechanism



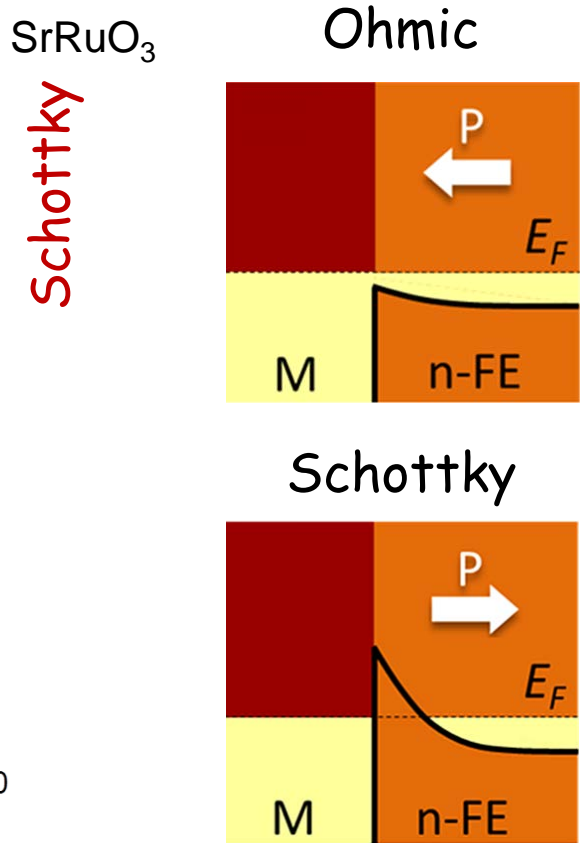
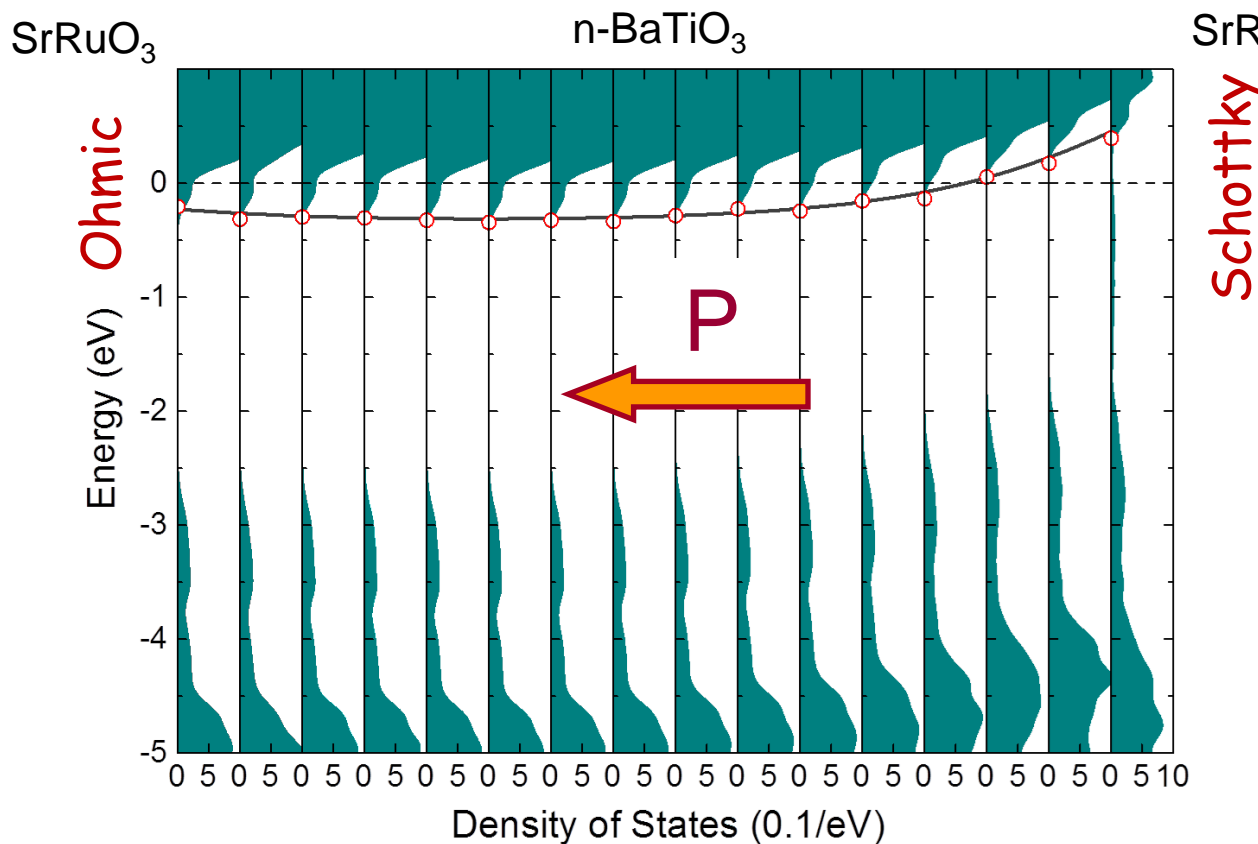
Metal/n-Ferroelectric Heterojunction



- Normal Metal:
Ferroelectric polarization dependent resistance
- Ferromagnetic Metal:
Ferroelectric polarization dependent spin-polarization

Band Bending across n-BaTiO₃

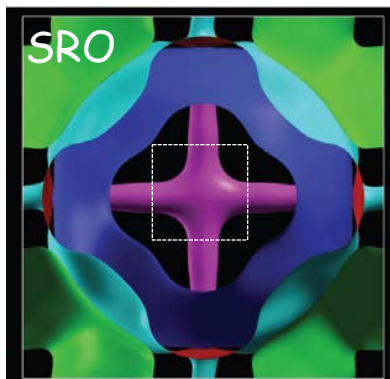
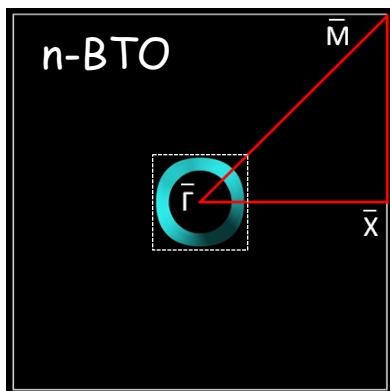
Liu et al., PRB 88, 165139 (2013)



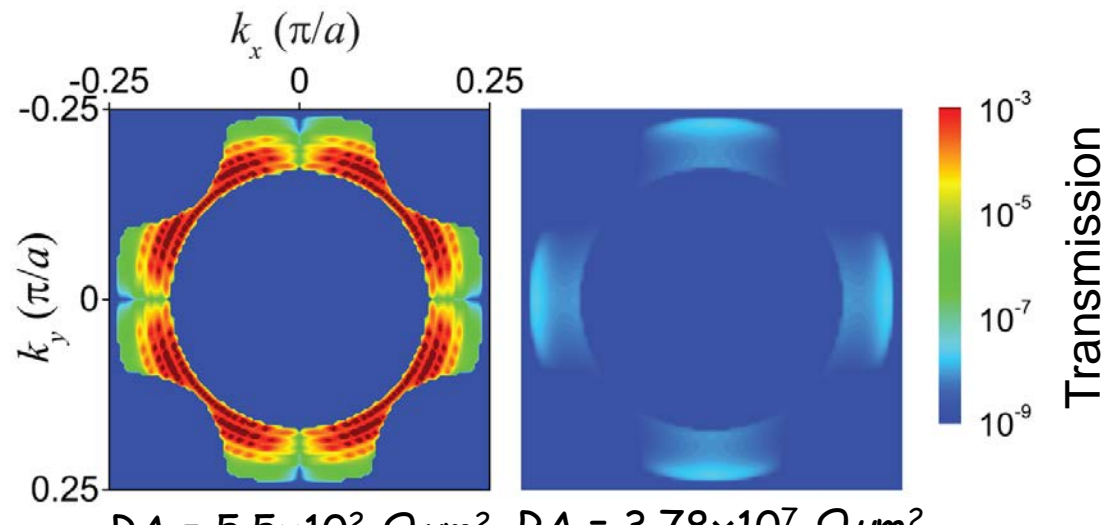
- Shottky or Ohmic contact depending on polarization orientation

Transmission

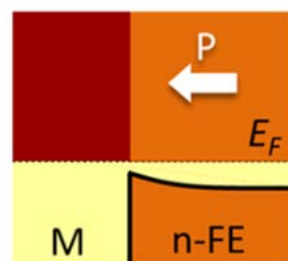
Fermi surfaces
(view along z-direction)



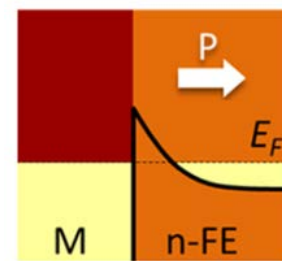
Liu et al., PRB 88, 165139 (2013)



Ohmic



Schottky



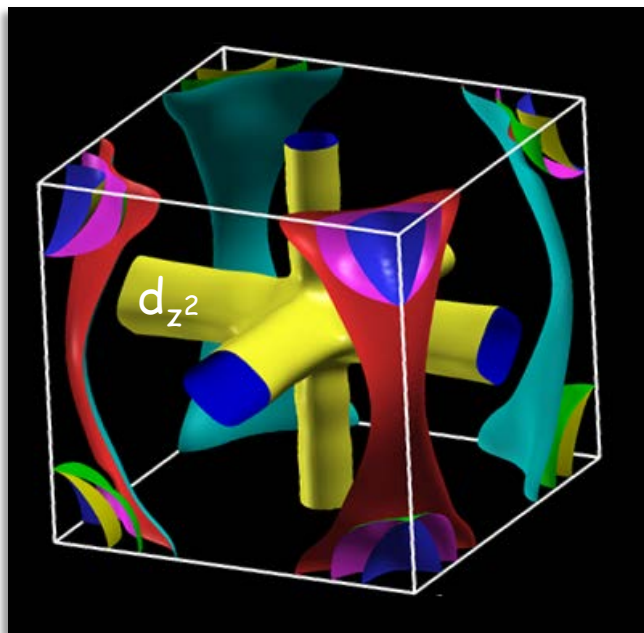
- 10^5 change in the interface resistance by switching ferroelectric polarization



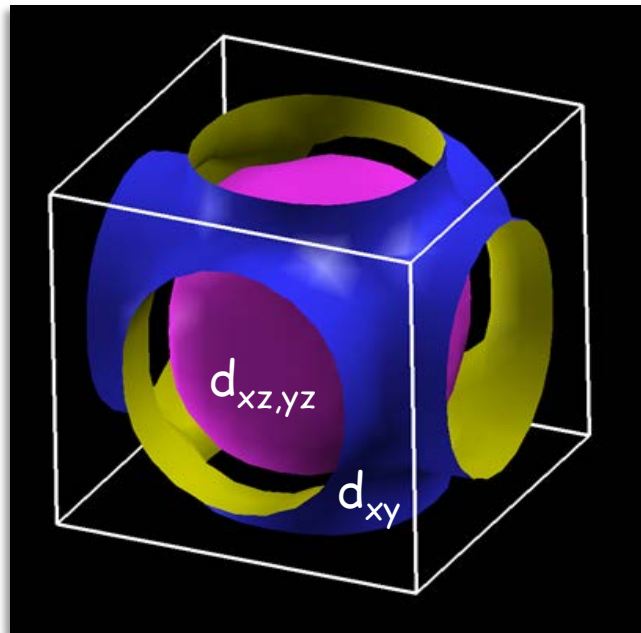
Fermi Surface of SrRuO₃

- SrRuO₃ is a ferromagnet below 160K
- Spin-dependent electric band structure ($1.2\mu_B/\text{f.u.}$)

Majority spin



Minority spin

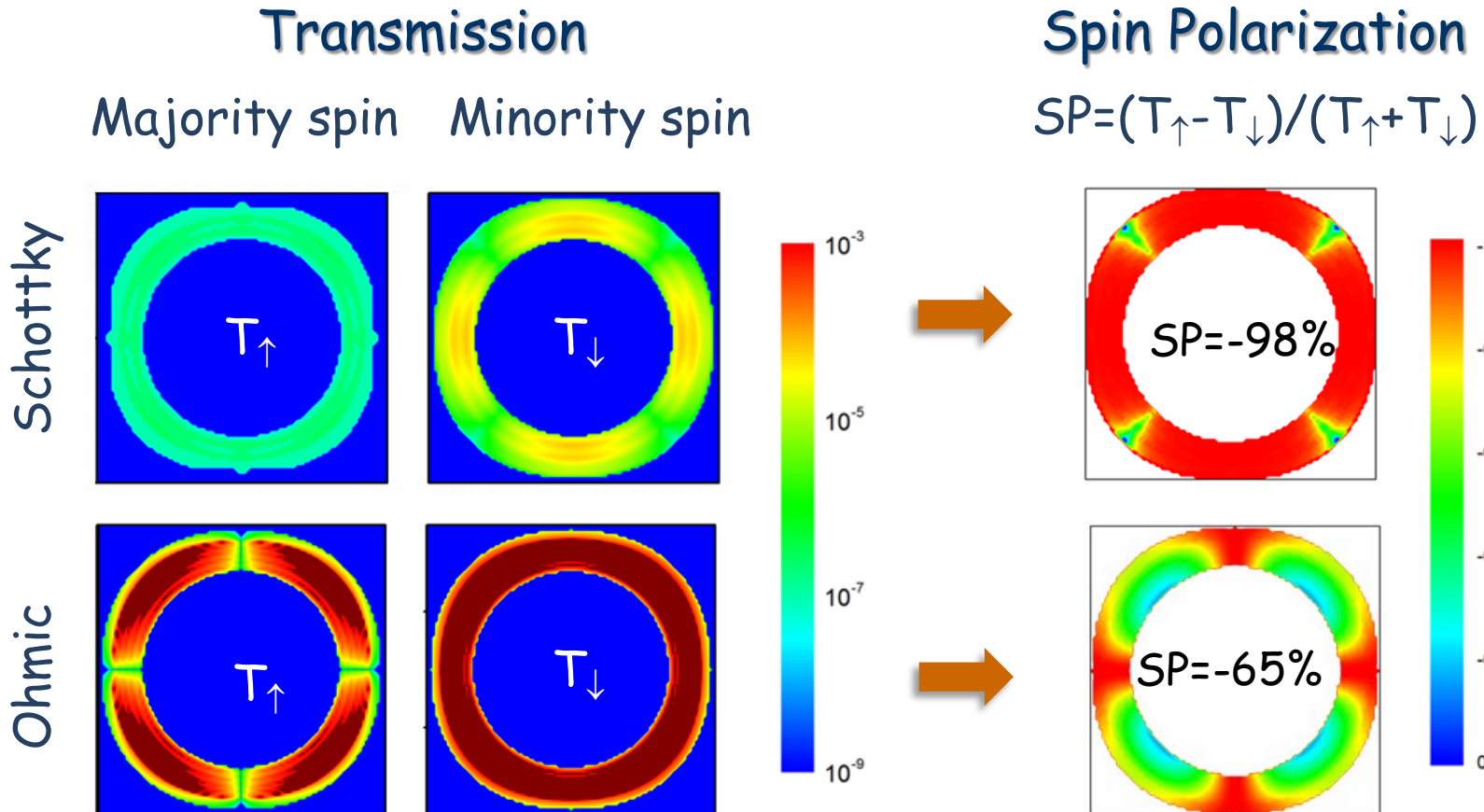


- Spin-dependent transmission is expected across SrRuO₃/n-BaTiO₃ interface



Transport Spin-Polarization

Liu et al., PRL 114, 046601 (2015)



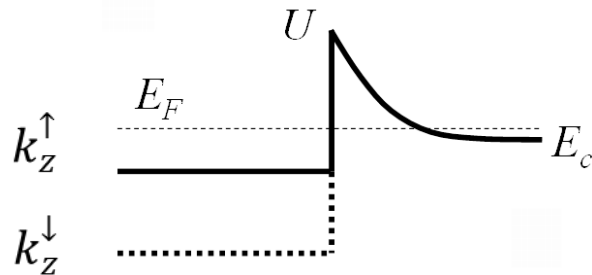
- Significant change in the transport spin-polarization with ferroelectric polarization reversal



Origin of Spin-Polarization Change

Liu et al., PRL 114, 046601 (2015)

A simple model:
Tunneling across a Schottky barrier



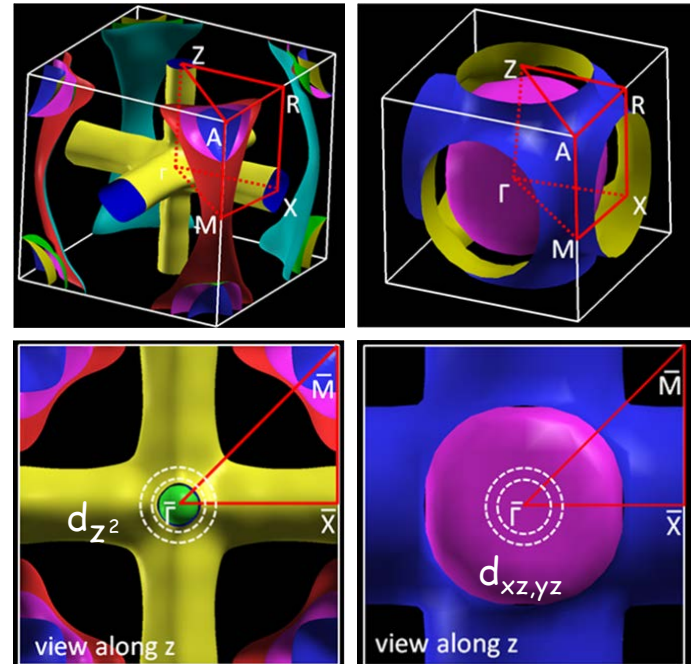
$$P_s = \left(\frac{k_z^{\uparrow} - k_z^{\downarrow}}{k_z^{\uparrow} + k_z^{\downarrow}} \right) \left(\frac{\kappa^2 - \gamma^2 k_z^{\uparrow} k_z^{\downarrow}}{\kappa^2 + \gamma^2 k_z^{\uparrow} k_z^{\downarrow}} \right)$$

κ - attenuation constant

similar to Slonczewski, PRB 39, 6995 (1989)

- Negative spin-polarization due to large minority-spin Fermi wave vector
- Change in the spin-polarization with ferroelectric polarization switching due to change in the barrier height
- Change in sign of the spin polarization for small electron doping

Fermi surface of SrRuO_3
Minority spin Majority spin



$$k_z^{\uparrow} \approx 0.079 \text{ \AA}^{-1} \quad k_z^{\downarrow} \approx 0.634 \text{ \AA}^{-1}$$



Conclusions

- Ferroelectric polarization provides a new degree of freedom to control materials properties relevant to spintronics
 - Interface magnetization
 - Interface magnetic order
 - Magnetocrystalline surface anisotropy
 - Electron and spin tunneling
 - Spin injection
- Switchable ferroelectric polarization at the interface with a magnetic metal forms a non-volatile spin-dependent state interesting for device applications



Acknowledgements

Theory:

U. Nebraska-Lincoln:

J. D. Burton, Xiaohui Liu,
Sitaram Jaswal

U. Puerto-Rico:

Julian Velev

East China Normal U.:

Chun-Gang Duan

Inst. Technology, India:

Manish Niranjan

U. Northern Iowa:

Pavel Lukashev

RAS, Moscow, Russia:

Mikhail Zhuravlev

ICTP, Trieste, Italy:

Alexander Smogunov

Erio Tosatti

Adv. Sci. Res. Center, Japan:

Sadamichi Maekawa

Experiment:

U. Nebraska:

Alexei Gruverman
Alexander Sinitskii

U. Wisconsin:

Chang-Beom Eom

Penn State:

YueWei Yin
Qi Li

U. Sci. & Tech. China, Hefei:

Xiao-Guang Li

Oak Ridge National Laboratory:

Young-Min Kim
Albina Borisevich
Stephen Pennycook

Seoul Nat. U.:

Sang Mo Yang
Tae Won Noh

Funding:

